UNIVERSITAT POLITÈCNICA DE CATALUNYA
BARCELONATECH
Escola d'Enginyeria de Telecomunicació
i Aeroespacial de Castelldefels

TREBALL DE FI DE CARRERA

TFC TITLE: Positioning in urban environments

DEGREE: Master in Aerospace Science and Technology

AUTHOR: Jan Sanromà Sánchez

ADVISOR: Jaume Sanz

SUPERVISOR: Olivier Julien

DATE: March 14, 2015

Title : Positioning in urban environments

Author: Jan Sanromà Sánchez

Advisor: Jaume Sanz

Supervisor: Olivier Julien

Date: March 14, 2015

Overview

This thesis will try to further increase the accuracy of a mixed GNSS and inertial solution for navigation in urban areas. The mix will represent a set of low cost sensors to measure their performance. The objectives will be the implementation of a multi-constellation GNSS receiver, and the research and test of modelling techniques for GNSS measurements based on carrier-to-noise ratio. Any other technique that allows for an increase in the accuracy will also be used and tested.
The laboratory work for this thesis will be done at l'Ecole Nationale de l'Aviation Civile as part of an exchange program. First of all the theoretical studies will be carried out, first of stand-alone GNSS and INS navigation and then on their integration. This integration will consist on the use of a Kalman Filter algorithm, and therefore additional theory on the implementation of this filter will be necessary. Then the current algorithm developed by ENAC is analysed, together with the hardware connection requested with the different equipment.
A measurement campaign was done to collect new samples from ENAC at the outskirts of Toulouse to the city center. Data was then post process several times to obtain the most optimal configuration for the receiver in urban and suburban environments. The results showed that the implementation of GLONASS together with the suggested weighting modelling based on carrier-to-noise level measurements allowed an increase of almost 50% in the accuracy of the position and the estimation of the yaw.

CONTENTS

LIST OF FIGURES

LIST OF TABLES

INTRODUCTION

Motivation

The number of Global Navigation Satellite Systems (GNSS) receivers has vastly increased in the past years. The constant reduction in price, cost and consumption of small, single frequency receivers has allowed an entire industry of production of cheap receivers for the mass market. Nowadays all mobile phones carry at least a Global Positioning System (GPS) receiver. Some are beginning to carry also a Globalnaya Navigatsionnaya Sputnikovaya Sistema (GLONASS), its Russian equivalent.

These receivers offer a good enough estimation of the user's position for most applications. In open sky areas, accuracy can go down below 5 meters, which is more than enough for most applications and Location-Based Services. In urban areas, due to the presence of tall buildings, accuracies can be highly degraded, causing the receiver to estimate its position with an error of tens of meters or more. In some cases the receiver is not even able to calculate the position at all due to the lack of visible satellites in the sky.

Due to the expansion of smart phones, inertial sensors like gyroscopes and accelerometers are also starting to reduce their prices, making them more accessible to the average user. Although navigation grade sensors, capable of outputting an Inertial Navigation Solution (INS) are still expensive, the trend is toward cost reduction.

Objectives

This thesis will try to further increase the accuracy of a mixed GNSS and INS sensors for use in urban areas. It will work on an already existing positioning and sensor integration algorithm developed by ENAC in order to overcome the different problems present in positioning in urban areas. This algorithm included already GNSS, INS and the use of a camera for sky detection.

The problem of increasing the accuracy of the solution will be treated from two different points of view. First it will be attempted to add more constellations to the algorithm, increasing from GPS only to GLONASS, Galileo, Beidou and EGNOS. As in a city environment only a small portion of the sky is visible, the objective is to be able to process as many satellites as possible.

The second topic of research will be the use of weighting schemes specific for urban environments: Use of carrier to noise measurements from the satellites in order to extrapolate and model the accuracy of the readings. This will allow to cancel noisier and inaccurate satellites that might degrade the position solution.

Structure

The structure of this report is as follows:

- Chapter 1 will introduce the different navigation principles, methods and sensors used for this thesis: GNSS and inertial navigation, setting the theoretical bases.
- Chapter 2 introduces the Kalman filter, the estimation algorithm used to compute a position solution from the measurement data.
- Chapter 3 will explain the existing state of the art. The current positioning and integration algorithm and the sensors used in the measurement campaigns.
- Chapter 4 shows and explains the different changes proposed to the algorithm in order to increase its accuracy and efficiency.
- Chapter 5 presents the results obtained in the measurement campaign.
- Finally, the conclusions of the thesis will be presented.
- Appendix A, containing the tables and figures of the results.

CHAPTER 1. NAVIGATION PRINCIPLES

Navigation is the field of study of the movement of vehicles from a place of origin to a destination. The objective then is to know where we are now (positioning) and how to reach our destination (guidance). Navigation systems will be anything that helps in that effort. Over the years several methods have existed : Landmarks can be used for navigation with the help of a map and a compass, to find the position of an object relative to those landmarks. In the ocean, where no landmarks are available, stars were used in order to find the current position and heading. These methods, as simple as they are, have been used for centuries in order to navigate the Earth.

These methods relay on visual clues in order to know a position, whether a star or a mountain, and while stars offer global coverage, maps very rarely cover the whole Earth with enough resolution. Already we are getting a sense of requirements that navigation systems must have in order to become more reliable and accurate.

In this chapter we will first introduce the reference systems used. Then, an explanation of the two most used navigation systems: GNSS and INS.

1.1. Coordinate Frames

Before introducing the navigation systems, we will briefly introduce the different references by which one can express the user's position. This small introduction will be useful for introducing GNSS and INS systems and their integration, as they both work with different references.

1.1.1. Earth Reference Frames

In order to represent position on Earth, three different possibilities exist:

- Earth-Centered Inertial (ECI)
- Earth-Center Earth-Fixed (ECEF)
- Local navigation frame

The ECI frame is centred at the Earth's center of mass, with the Z axis pointing to the north pole and the X and Y axes lying at the equatorial plane pointing at fixed stars. The ECEF frame shares the definition for the Z axis, which points to the north pole. The X axis however points toward the intersection of the Greenwich meridian and the equatorial plane. The Y axis is set at 90° from the Z and X axes. The difference between the two systems is that ECI is not fixed and takes into account the rotation of the Earth. Following the convention in [1] ECI frame will be reference by the superindex i and ECEF coordinates by the superindex e

A local navigation frame is defined by a relative position between two points. Usually this distance is defined in three axis East, North, Up (ENU). The local frame can offer absolute

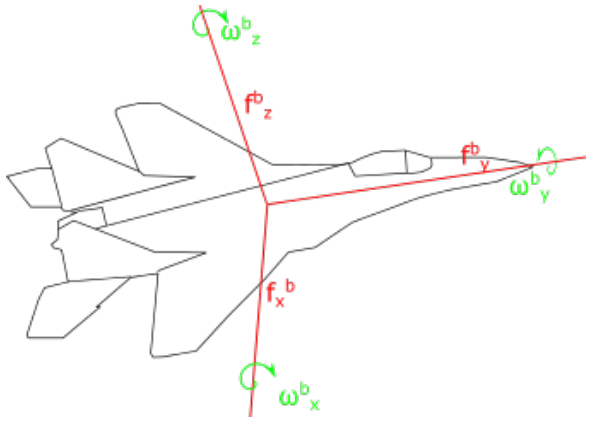

Figure 1.1: IMU measurements on axis

positioning as long as the absolute position of one of the two objects is known. Conversion between the three systems is done easily, the formulas being available in [1].

As for the shape of the Earth different references are used. Each one considers different center of mass for the Earth and have a different conception of the Earth surface. The most extended one is WGS-84 [2], which is the one used by GPS and many applications. The coordinate frames used by other GNSS systems differ a few centimetres from the GPS[3] frame and they do not need to be taken into account unless high accuracy is wanted.

1.1.2. Body Frame

In a body reference frame the origin of axes is placed in the body, and the direction of the axes is also set around the body. Figure 1.1 shows this type of reference where f is used to represent acceleration along the axis and ω to represent rotations. The superindex b will be used in following sections to indicate a body frame.

Accelerometers and gyroscopes traditionally output their data in this format.

1.2. Global Navigation Satellite System

Global Navigation Satellite Systems (GNSS) ideas started at the beginning of the space race as a way to improve on current, land based navigation systems. The idea behind GNSS is to put a satellite in orbit which, by the use of radio wave signals, allows a user to compute its position in the globe. A satellite, unlike a land-based system, offers easy global coverage, as it is orbiting the Earth. A simple analogy is that one can see a tall lighthouse easier than a smaller one. If the lighthouse is 20000 Km tall in space, it could be seen from half a world away. [4]

GPS is currently the most widely used navigation system worldwide. It offers global, all weather, limitless coverage. Together with the Russian system GLONASS, the European Galileo and the Chinese Beidou, they form the GNSS systems. They all rely on the same principle of functioning, called trilateration. Minor differences between the systems are commented in Section 1.4..

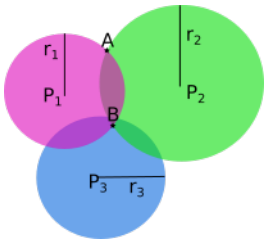

Figure 1.2: Lateration principles on 2D plane

1.2.1. Lateration

The principle of lateration is to find the position of an object relative to a set of references by knowing the distance between them. An example of this method in a 2D plane can be seen in Figure 1.2. In this example, two references are used, called $P1$ and $P2$, whose position is well known. By knowing the distances $r1$ and $r2$ between those two references to the receiver we can plot two circles, corresponding to the green and pink circles. The receiver is therefore in the intersection of those two circles, either in point A or point B. A third reference $P3$ would be needed to solve this ambiguity. For the case of GPS this ambiguity can be solved just by imposing that the point is close to the Earth surface, as the other point will be in deep space.

For a 2D space with two unknowns, we need two reference points (or satellites in the case of GNSS). Moving this example to a 3D space, we obtain that in order to known our position both in a horizontal and vertical planes we need at least three satellites (one for each unknown). However, the method by which GPS estimates the distance to the satellite will introduce a new unknown and therefore another satellite, totalling four.

1.2.2. Pseudoranges

GNSS systems are able to find their position on Earth by constantly calculating the distance between a reference (a satellite) and the receiver. This distance is calculated by means of a method called Time of Arrival (ToA). The concept is quite simple: The satellite transmits a signal at a specified known instant. The signal then travels through space and arrives at a receiver, which takes notice of the current time. Since we know at which time the satellite started transmitting and we know at which time we received the signal we can calculate the Time of Flight ΔT, and since radio signals travel at the speed of light c, we can compute the true range d as :

$$d = \Delta T \cdot c \tag{1.1}$$

This method requires very accurate time measurements, as an error of 1 microsecond in timing becomes 300 m in position error when multiplied by the speed of light. The clock in the satellite is an atomic clock capable of extreme accuracy, but the one in the receiver is not. It is, by easiness of design and manufacture, a cheap clock that drifts heavily from the true time frame, in the order of seconds in a day. The difference between the receiver clock and the reference time frame is called receiver clock error or bias (indicated as δt_r), and it becomes another unknown to be solved in the system. Since this receiver clock error is common to all measurements, it is easily included in the Equation 1.1 as :

$$\rho = d + \delta t_r \cdot c \tag{1.2}$$

Once we include the receiver clock error δt in the computation we no longer talk about range, but rather about pseudorange ρ, as it is the range as perceived by the receiver and it includes the clock bias. This method allows for a cheap clock to be built in the receiver, reducing greatly manufacturing costs and allows for a very easy system for synchronizing clocks globally. The expense is that an additional satellite is required for positioning. Another clock error is present in the satellite, but it is estimated by the control segment and transmitted to the user [5].

1.2.3. Linearization

In order to compute a position the receiver must merge the information of the satellite's position and the pseudorange to compute a solution. The geometric definition of pseudorange in ECEF coordinates is:

$$\rho = \sqrt{(r_{sat} - r_r)^2} + \delta t \cdot c = \sqrt{(x_{sat} - x_r)^2 + (y_{sat} - y_r)^2 + (z_{sat} - z_r)^2} + \delta t_r \cdot c \tag{1.3}$$

The system of equations to be solved for four or more satellites becomes:

$$\begin{cases} \rho_1 = \sqrt{(x_1 - x_r)^2 + (y_1 - y_r)^2 + (z_1 - z_r)^2} + \delta t_r \cdot c \\ \rho_2 = \sqrt{(x_2 - x_r)^2 + (y_2 - y_r)^2 + (z_2 - z_r)^2} + \delta t_r \cdot c \\ \rho_3 = \sqrt{(x_3 - x_r)^2 + (y_3 - y_r)^2 + (z_3 - z_r)^2} + \delta t_r \cdot c \\ \rho_4 = \sqrt{(x_4 - x_r)^2 + (y_4 - y_r)^2 + (z_4 - z_r)^2} + \delta t_r \cdot c \end{cases} \tag{1.4}$$

Where:

- $r_{sat} = (x_{sat}, y_{sat}, z_{sat})$ is the satellite position.
- $r_r = (x_r, y_r, z_r)$ is the receiver position.

In this equation our estimate (x_r, y_r, z_r) are hidden inside of a square root. To solve this set of non linear equations we must linearise the Equation system 1.4. In that direction we take the first order Taylor series expansion of 1.3 at an estimated nearby point $\hat{r}_u = (\hat{x}_r, \hat{y}_r, \hat{z}_r)$ and estimated clock error $\delta\hat{t}_r$. The super index $\hat{}$ is used to denote estimated.

$$\rho = \hat{\rho} - \frac{x_{sat} - \hat{x}_r}{\hat{d}_r}\Delta x - \frac{y_{sat} - \hat{y}_r}{\hat{d}_r}\Delta y + \frac{z_{sat} - \hat{z}_r}{\hat{d}_r}\Delta z + \Delta t_r \cdot c + \varepsilon \tag{1.5}$$

Where $\hat{\rho}$ is the pseudorange that should be by a estimated receiver at $\hat{r}_r$ and $\hat{d}_r$ being the true geometric range to point $\hat{r}_r$. Other additional error sources and lienariztion errors are include in the parameter ε.

$$\hat{\rho} = \hat{d}_r + \delta\hat{t}_r \cdot c \tag{1.6}$$

$$\hat{d_r} = \sqrt{(x_{sat} - \hat{x}_r)^2 + (y_{sat} - \hat{y}_r)^2 + (z_{sat} - \hat{z}_r)^2} \tag{1.7}$$

The distance between the true and estimated position $\Delta r = r_r - \hat{r}_r$ is expressed as:

$$\Delta x = x_r - \hat{x}_r \,;\, \Delta y = y_r - \hat{y}_r \,;\, \Delta z = z_r - \hat{z}_r \,;\, \Delta t = \delta t_r - \delta \hat{t}_r \tag{1.8}$$

If we then calculate the pseudorange difference $\rho - \hat{\rho}$ between the true receiver position r_r and an estimated point $\hat{r}_r$ for an n number of measurements we obtain the following set of equations:

$$\begin{pmatrix} \rho_1 - \hat{\rho}_1 \\ \rho_2 - \hat{\rho}_2 \\ \vdots \\ \rho_n - \hat{\rho}_n \end{pmatrix} = \begin{pmatrix} \frac{x_1 - \hat{x}_r}{\hat{d}_1} & \frac{y_1 - \hat{y}_r}{\hat{d}_1} & \frac{z_1 - \hat{z}_r}{\hat{d}_1} & 1 \\ \frac{x_2 - \hat{x}_r}{\hat{d}_2} & \frac{y_2 - \hat{y}_r}{\hat{d}_2} & \frac{z_2 - \hat{z}_r}{\hat{d}_2} & 1 \\ \vdots & \vdots & \vdots & \vdots \\ \frac{x_n - \hat{x}_r}{\hat{d}_n} & \frac{y_n - \hat{y}_r}{\hat{d}_n} & \frac{z_n - \hat{z}_r}{\hat{d}_n} & 1 \end{pmatrix} \begin{pmatrix} \Delta x \\ \Delta y \\ \Delta z \\ \delta t \cdot c \end{pmatrix} + \varepsilon \tag{1.9}$$

Which rewritten using matrix notation becomes:

$$\Delta\hat{\rho} = H\Delta r + \varepsilon \tag{1.10}$$

Where H is the measurement matrix containing all the partial derivatives to all satellites, or the unitary vector to all satellites in the three dimensions. If H contains measurements to only four satellites, it can be easily inverted to obtain a solution, yet most of the time it contains a different number. Considering then that the measurement matrix cannot be inverted if there are more than four satellite available, the Least Squares Solution to the system becomes:

$$\Delta\hat{x} = (H^T R^{-1} H)^{-1} H^T R^{-1} \Delta\hat{\rho} \tag{1.11}$$

Where R is a square matrix weighting each of the measurements. Section 5 explains the composition of the R matrix further.

With equation 1.11 we can obtain a solution using the satellites measurements. All additional errors in ε however force it to be solved in several iterations in order for the solution to converge. The method also requires an initial position to be used. The distance between the reference point and the real position can be very high, as the solution will converge very quickly.

1.2.4. Pseudorange Rate

So far we have talked of pseudorange measurements and how they are used to find a position, yet speed can also be obtained from GPS measurements. As speed v_r is the time derivative of position r_r, pseudorange's ρ time derivative creates a new measurement called pseudorange rate $\dot{\rho}$.

One way to compute the pseudorange rate is to compute the increment of pseudorange from one iteration to the next. Although this method is valid, it is going to be very random, as noise is accumulated in pseudorange measurements. The best way to compute

pseudorange rate $\dot{\rho}$ is by means of the Doppler frequency shift. The Doppler shift relates the relative speed of a transmitter (the satellite) and a receiver in an accurate way. From Doppler readings (which are generated in any GPS receiver as part of the demodulation of the carrier) one can estimate the pseudorange rate, and the user's speed.

The Doppler effect's frequency shift D can be defined using the following formula:

$$f_D = f_0(1 - \frac{\vec{u} \cdot \Delta\vec{v}}{c}) \tag{1.12}$$

Where:

- f_D is the frequency shift.
- f_0 is the central frequency of the signal (1575.42 MHz for GPS)
- $\vec{u}$ is the unitary vector from satellite to receiver.
- $\Delta\vec{v}$ is the increase of speed between satellite and receiver

Similarly to the pseudorange ρ having a component due to the receiver clock bias δt , the pseudorange rate $\dot{\rho}$ has a component caused by the clock drift $\delta\dot{t}$ such that:

$$f_D = \hat{f}_D(1 + \delta\dot{t}) \tag{1.13}$$

Where $\hat{f}_D$ is the Doppler shift as measured by the receiver. Taking that into account, the pseudorange rate $\dot{\rho}$ equation becomes:

$$\dot{\rho} = -\frac{\hat{f}_D \cdot c}{f_0} - \vec{u} \cdot \Delta\vec{v} + \delta\dot{t} \cdot c \tag{1.14}$$

The unitary vector can be computed using the following formula:

$$\vec{u} = \frac{r_{sat} - r_r}{d} \tag{1.15}$$

Where:

- r_{sat} is the satellite position.
- r_r is the receiver position.
- d is the geometric distance between them.

This definition of $\vec{u}$ is the exact same as the components of the H matrix in 1.9. Therefore both pseudorange and pseudorange rate equations can be solved using equation 1.11. The system of equations for solving both the user's position and velocity becomes:

$$\begin{pmatrix} \Delta\rho_1 \\ \vdots \\ \Delta\rho_n \\ \Delta\dot{\rho}_1 \\ \Delta\dot{\rho}_n \end{pmatrix} = \begin{pmatrix} u_{x,1} & u_{y,1} & u_{z,1} & 0 & 0 & 0 & 1 & 0 \\ \vdots & \vdots & \vdots & \vdots & \vdots & \vdots & \vdots & \vdots \\ u_{x,n} & u_{y,n} & u_{z,n} & 0 & 0 & 0 & 1 & 0 \\ 0 & 0 & 0 & u_{x,1} & u_{y,1} & u_{z,1} & 0 & 1 \\ \vdots & \vdots & \vdots & \vdots & \vdots & \vdots & \vdots & \vdots \\ 0 & 0 & 0 & u_{x,n} & u_{y,n} & u_{z,n} & 0 & 1 \end{pmatrix} \begin{pmatrix} \Delta x \\ \Delta y \\ \Delta z \\ \Delta\dot{x} \\ \Delta\dot{y} \\ \Delta\dot{z} \\ \delta t \\ \delta\dot{t} \end{pmatrix} + \varepsilon \tag{1.16}$$

Where:

- $u_{d,i}$ is the unitary vector at dimension x, y or z for satellite i.
- n is the number of satellites available at that instant.
- ε is a matrix including all additional error sources.

The full navigation equation (1.16) can then be solved using the WLSE method 1.11, taking into account that matrix R must now include the covariance of the Doppler measurements as well as the pseudorange measurements. Equation 4.7 contains the definition of the covariance matrix.

1.3. GNSS Errors

So far we have explained the ideal principles of GNSS positioning. In real life however measurements are highly affected by errors, which reduce the accuracy of the PVT solution. These additional errors, which in previous equations were included in vector ε can disrupt the solution several hundred meters. Different types of errors affect the GNSS measurements, as any delay in the signal or misplacement of the satellite will affect the time measurement and the pseudorange. An approximate error budget is :

- Ionospheric and tropospheric delay: Error caused by the influence of the Earth's atmosphere. (4 m and 1 m)
- Ephemeris errors: Errors in the computation of the satellite's position and clock bias. (2 m)
- Instrumental errors: Error caused by electrical noise present in both the satellite and the receiver. (0.5 m)
- Multipath: Reflection of signals by nearby objects.

Of all the errors affecting the measurements the main one to be covered in this thesis is multipath, as it is the main one affecting urban environments.

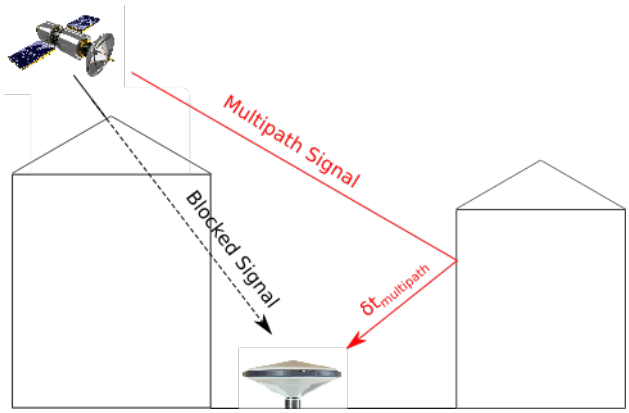

Figure 1.3: Multipath on an urban environment

1.3.1. Multipath

Multipath is one of the main errors in positioning and the biggest in urban environments. Multipath is the reflection of radio signal in surfaces near the user, creating echoes of the original signal that disrupt the receiver's readings. As GNSS are based on measuring the Time of Flight, any reflection will increase the signal travel time and increase the measured pseudorange. Most of the time the direct signal is much more powerful than the reflection. In that case the error caused by reflections is reduced as the receiver will track the most powerful signal. Multipath causes the biggest error when the direct signal is blocked like in the Figure 1.3. In this example, the direct signal is not received, also known as a non line of sight (NLOS) signal. The reflected signal (in red) is being tracked as the direct signal instead, since receiver is unable to tell them apart. This causes an increase in the measured pseudorange of $\delta t_{multipath}$, which depending on the geometry can account for several tens of meters.

In urban canyons multipath will account for the biggest positioning error 30 to 50 m of error being common. To reduce its effect the best option is to be able to tell LOS and NLOS satellites apart, so to limit the effect of reflected signals into the solution. Chapter 4 expands on the topic, while Chapter 3 describes the use of a camera to detect visible sky areas [6]

1.4. Constellations

GNSS include different constellations developed by the different countries over the years. The military implications of accurate navigation means that systems are not always interoperable and none of them give full free access to all of the possible messages. Currently four global systems exist: the American GPS and the Russian GLONASS already deployed and operational and the European Galileo and Chinese Beidou systems, still being launched. All of them however work on the same principles of lateration and the formation of pseudoranges from Time of Flight information.

1.4.1. Advantages of multiconstellation

As explained earlier, a minimum of four satellites is needed to obtain a position fix from a GNSS system based on lateration and pseudoranges, which correspond to the four unknowns (three for position plus the user clock time offset). Once a fix is obtained, tracking can be maintained with only 3 satellites as long as altitude is considered constant. By design, four GPS satellites at least are always visible from any point of Earth, as long as there are no obstacles in the line-of-sight. Special regions like cities or high latitude valleys might offer less cover, as direct view of the sky is blocked by obstacles. When this happens, the GNSS solution might be heavily degraded. No position solution will be output when not enough satellites are in view, creating gaps in the data.

Using a second constellation allows the user to effectively double the number of available satellites at any point on Earth, therefore increasing accuracy in low visibility areas. The addition of GLONASS specifically allows for much better positioning at high latitudes, as its orbits have a higher inclination, offering better coverage of polar regions. A new constellation however adds an additional unknown, as another clock bias must be estimated. This adds complexity to the algorithm.

It is very interesting to use as many constellations as possible in zones with low visibility like urban canyons. As more satellites are available, shortages in visibility are less likely. Also having more than four satellites increases the accuracy of the solution. Another interesting point of the use of several constellations is that as the number of satellites increases, they can be filtered in order to eliminate from the computation those satellite that degrade the most the solution, like NLOS satellites (Section 1.3.1.). Using a multi constellation configuration satellites can be excluded without risking having less than four visible satellites.

The following sections will cover the status, orbits, signals and messages of the four GNSS constellations and how likely they are to integrate with each other.

1.4.2. Global Positioning System

Global Positioning System GPS was the first deployed GNSS system and it is also the most widely used, with 2 billion users estimated. It is operated and maintained by the U.S Department of Defense. The GPS constellation consists of 32 satellites, giving full global coverage, guaranteeing that at least four satellites are visible in any open area around the globe.

As the first and most widely used system, GPS set the reference for future GNSS systems. Following is a list of its characteristics [4]:

a Signals

GPS satellites transmit two signals: the civil Coarse Acquisition (C/A) code and the military $P(Y)$ code, both used for determining the pseudorange between user and satellites. The P(Y) code is restricted to authorized users. Inside the C/A code, which is the most widely used, we find three components:

- A carrier: which contains no information.
- PRN code: the code used for ranging, identifying the satellite and spreading the signal against interference.
- Navigation message: containing the status of the constellation and the GPS time.

The position of the satellite is transmitted in the navigation message inside the ephemeris. In them are the Keplerian elements (Orbit inclination, excentricity, true anomaly,...), which can describe the position of the satellite in a orbit [7]. The full list of parameters, as well as algorithm to compute the satellite's position are given in the GPS Interface Control Document [8].

The navigation message also includes an almanac: A raw estimation of the position of the rest of the constellation. This almanac is used to speed up acquisition and reduce the search space. Parameters for the corrections of the ionospheric delay are also transmitted. The model for the ionospheric error is called Klobuchar, and it can correct up to 50% of the error.

b Frequencies

GPS operates in three aeronautical frequencies described in Table 1.1. The use of several frequencies allows redundancy against jamming for military uses and the possibility to remove the ionospheric errors [9]. Only users of the military $P(Y)$ code are capable of reading the information of the $L2$ frequency band. For the purpose of this thesis, only L1 C/A coarse is used, as it is the one used by most of the receivers. Dual frequency receivers can achieve high levels of accuracy but tend to cost in the order of thousands of Euro.

Table 1.1: GPS frequency bands

Band	Frequency
L1	1575.42 MHz
L2	1227 MHz
L5	1176.45 MHz

c Multiple access

All GPS satellites transmit at the same frequency at the same time. In order to identify and separate each signal, each satellite transmits a special code, called Pseudo Random Noise (PRN) that allows the user to decode and demodulate the signal of each individual satellite. GPS then uses a form of Code Division Multiple Access (CDMA). Since each satellite has a unique PRN code, that does not correlate with any other, PRN is the word used to identify satellites.

1.4.3. Globalnaya Navigatsionnaya Sputnikovaya Sistema

The Globalnaya navigatsionnaya sputnikovaya Sistema (GLONASS) was the equivalent GNSS system developed in the old Soviet Union from 1976. Launches started at 1982,

achieving full constellation (24 satellites) in 1995. The short life-span (only three years) of the early launched satellites together with the economic collapse of the Soviet Union meant that the system was not properly maintained. In the early 2000's the system was modernized and restored. A new satellite, the GLONASS-M was introduced, expanding the lifetime from 3 to 7 years. By 2010 the constellation was refilled, being the second fully functional GNSS system in orbit. [10]

1.4.3.1. Characteristics

GLONASS works as a trilateration system as GPS. It also uses a ranging code mixed with a longer navigation message that contains information on the orbit status. It transmits in two frequencies, which allows it to estimate and cancel the ionospheric effect. However, since it was designed during the cold war, it was not intended to work in conjunction with GPS. Substantial differences exists that make the merging and fusion of the two systems complicated, which results in an increased price. For cheap, mass-market receivers, this usually discards GLONASS. However this trend is slowly changing, and many smart phones include now a two-constellation receiver.

The newest version of GLONASS satellites (GLONASS-K) are developed with some compatibility in GPS in mind, making the merge of systems easier for manufacturers. However, as of 2014 only 2 GLONASS-K are operational, the constellation being dominated by GLONASS-M satellite, which maintain a number of critical differences with the GPS, mainly being:

- Time reference
- Orbits and information on the navigation message
- Frequency of operation
- Maximum received power
- Signals transmitted
- Datum used

This characteristics will be described next, with a more practical approach to how to overcome these differences seen in Section 4.1..

a Time reference

GLONASS uses UTC(SU) as its time frame, the SU abbreviation meaning that it is UTC as tracked from Russia. UTC differentiates from GPS time (GPST) in the number of leap seconds introduced to correct between the difference of sidereal and solar days. This difference includes an integer number of seconds (16 leap seconds by Autumm 2014) plus a non integer difference caused by the different tracking systems.

b Orbit and navigation message

GLONASS operates at a slightly lower orbit than GPS at around 19000 km from Earth. Satellites are divided in three orbital planes like GPS, but the inclination of these orbit is 10° higher, allowing GLONASS to cover higher latitudes than GPS.

These orbital parameters are transmitted together with the ranging C/A code in the navigation message. Unlike GPS, the parameters needed to compute the satellites position at any given time are not transmitted using Keplerian elements, but rather using Cartesian parameters. These parameters can be integrated over a time span to obtain the satellite position at any given time. The ephemeris are updated by the control segment every 30 minutes. The total accuracy obtainable from the ephemeris is lower than that of GPS [11]. The GLONASS navigation message does not include any Klobuchar parameters (the model used to estimate ionospheric effect). Relativistic corrections are transmitted inside the satellite clock correction parameters.

c Frequency and FDMA

GLONASS operates in two frequencies L1 and L2 (A third fequency L3 is also being used by the new GLONASS-K satellites) that allow it to compute and correct the ionosphere delay. These frequencies, however close, are not identical to GPS's L1 and L2 as seen in Table 1.2 . For this reason they are often called G1 and G2, to differentiate with GPS bands. An additional frequency L3 is being transmitted by the new GLONASS-K satellites, which includes new, modernized signals.

Table 1.2: GLONASS frequency bands

Band	Frequency
L1	1602 MHz
L2	1247 MHz
L3	1205.140 MHz

Unlike GPS, GLONASS doesn't use PRN codes to differentiate between satellites, but rather uses a different frequency and the same PRN code for all satellites. This type of division, known as Frequency Division Multiple Acces (FDMA) is the same one used to separate channels in commercial radio. Each satellite will transmit by a multiple of the original L1 band, therefore when the receiver tracks a signal it can recognize the emitting satellite by looking at the frequency band.

d Maximum received power

GLONASS ICD document [10] describes the maximum received power on the surface of the Earth. This curve is lower in the case of GLONASS than of GPS, meaning that GLONASS received power will be always lower in the same elevation conditions, around 3 dBHz. Figure 1.4 represents this difference in a graphic comparing received power and elevation for GPS (top) and GLONASS (bottom)

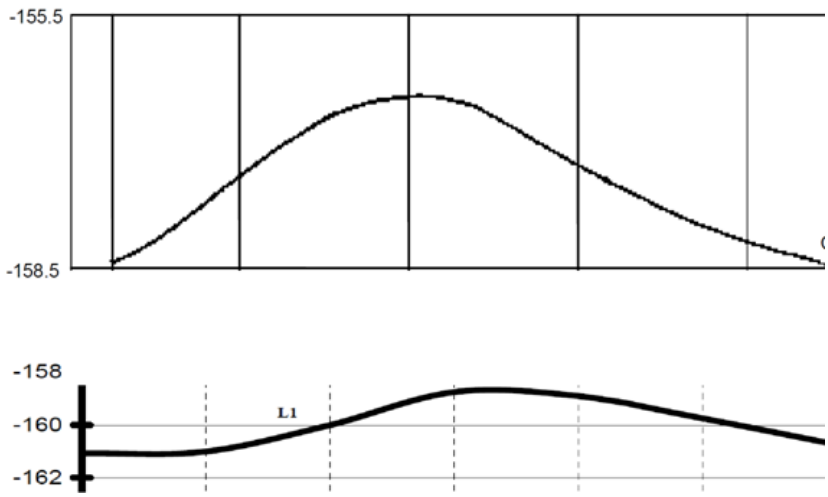

Figure 1.4: Graphs showing received power depending on elevation. Top : GPS, Bottom: GLONASS[10] [8]

e Datum

GLONASS uses the PZ90 datum rather than WGS84, therefore all satellite positions (and therefore any fix the receiver obtains from them) are offset between the two systems. In 2014 the Russians updated the datum to Pz90.11, which has centimetre level offset from WGS84.[3]

1.4.4. Galileo, Beidou

The newest GNSS systems to be developed are the European Galileo and Chinese Beidou systems. Currently in the deployment state, they both aim to give their respective countries independence from the American and Russian systems.

Initially, Galileo was meant to be a joint Chinese and European system, with the Chinese developing their own augmentation system COMPASS (equivalent to the European EGNOS). Political problems meant that both systems followed different deployment [12].

Unlike GLONASS, which was not meant to cooperate with GPS, both Galileo and Beidou were designed with integration with each other and GPS, trying to reduce to a minimum the differences and maximizing the similarities. In that sense the characteristics of both systems are.

f Frequency

Galileo, Beidou and GPS share all the same frequency band at L1. This means that a single antenna can cover all the systems, avoiding the problems with the RF front-end that GLONASS has.

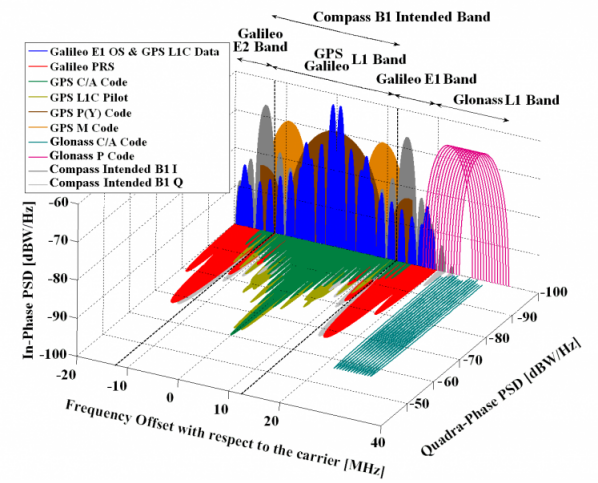

Figure 1.5: All GNSS signal on the L1 band [13]

g Modulation

GPS uses Binary Phase Shift Keying (BPSK), which in the frequency domain creates a signal in which most of the power is concentrated in the central frequency. In order to avoid interference, both Galileo and Beidou transmit with different modulation, so that the signal do not exactly superpose. The distribution of signals in the frequency domain can be seen in Figure 1.5. It can be appreciated that even though the signal share the same band, they are all shaped differently due to their modulations in order to further reduce interference.

h Inter system time

Galileo and Beidou include information of their time difference with GPS in their navigation messages. This means that no new unknowns need to be added to the Kalman filter, therefore no computing load is added to the navigation filter. [14] [17]

1.5. Inertial Navigation Systems

Inertial navigation systems (INS) are navigation systems capable of finding a user's position based solely on measurements of the inertial forces of the vehicle. INS measure mainly accelerations from an accelerometer and rotation rate from a gyroscope. This measurements are taken purely from the inertial reactions of any motion and they are not based on any external reference. A navigation solution can be obtained from inertial measurements by integrating the accelerations and angle rates to obtain a velocity estimation first, and then integrate it again to obtain a position.

This section will cover the specifics of Inertial measurements and the equations that allow inertial navigation. [1]

1.5.1. Inertial Measurements

Inertial measurements come from two main sensors: accelerometers and gyroscopes. An accelerometer measures linear acceleration on its three main axes, while a gyroscope will measure rotation rate around those axes. Both sensors are then combined into an Inertial Measurement Unit or IMU. The IMU generates inertial data reading which can then be input into the navigation equations in order to obtain a navigation solution.

The main properties of an IMU are as follows:

- Accelerometers are noisy, as they measure any vibration in the vehicle.
- Gyroscopes are not noisy, but their output drifts away very quickly.
- Accelerometers can use gravity as a reference, but their high level of noise does not make them suitable as the output must be filtered, which causes a delay in the output.
- Gyroscopes cannot reference their values to anything, they can only measure change from the original attitude. Any drift present tends to accumulate, deviating the solution very quickly unless corrected by other means (like the accelerometers).

Based on this list of properties it makes sense to combine accelerometer and gyroscopes in order to obtain the best of each. Accelerometers can be used to correct for the gyroscopes drift while at the same time obtain the quick response of the gyroscope.

Inertial navigation works by integrating the accelerations in order to obtain a position. This process is also called dead reckoning (DR). Simply put, dead reckoning works by prolonging the current speed and acceleration a certain amount of time to obtain a position. The system has to be initialized at a known location, and from there on theoretically it should be possible to navigate without any external reference. In reality however, this is not close to possible, as errors will start to accumulate over time with the integration, the position drifting quickly from the true one as errors accumulate. If a purely Inertial solution is used, it is not possible to correct for these drifts, as by definition no external reference is used.

Based on the amount of drift, several categories of IMU can be made:

- Aviation Grade: 1.5 km of drift in the first hour of navigation , used in aeroplanes and submarines and costs 100000 Euro .
- Tactical grade: Useful for a stand alone solution for a few minutes only. They can cost around 1000 Euro .
- Consumer grade: Not useful for navigation, as the solution drifts by several meters per second. They can be found in cell phones and cars and cost a few Euro.

The drifts in the IMU influence deeply its range of uses, limiting its accuracy to a minute or so for the cheapest solution. IMUs however have several advantages: they can produce output at several time per second, they do not need any external help and they can measure the vehicles attitude, not only position. Subsection 1.5.2. will cover the equations to obtain a navigation position using inertial measurements, while Section 3.1. will cover methods of increasing the performance of IMU by combining it with a GNSS.

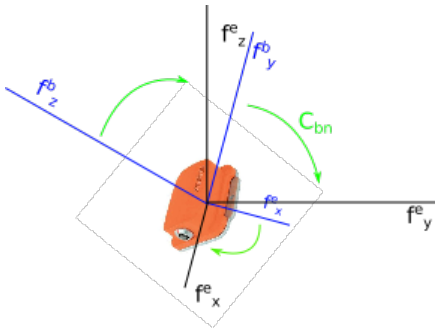

Figure 1.6: Specific force frame transformation

1.5.2. Navigation Equation

In order to translate the IMU raw measurements of acceleration and angular rate into a position, velocity and attitude (PVA) solution several equations are required. These are known as the IMU mechanization, or navigation equations.

The first step in the computation of navigation is to obtain the attitude of the mobile. The attitude is stored in the rotation matrix C_{bn} which includes the required rotations to express a body's attitude. Figure 1.6 shows this rotation from the axis centered around the IMU f^b, to the earth referenced axis f^e, where the Z axis is always aligned with gravity. This transformation is required to have stable axis that do not change constantly.

The rotation matrix C_{bn} is computed as an update from the previous estimated attitude. The angular rate information is used to update the attitude in the time interval. The formulas to obtain the rotation matrix can be found in [1]:

As seen in figure 1.6 a rotation matrix allows for a change from a local reference frame f^b_{ib} to an Specific Force frame f^e_{ib} by Equation 1.17.

$$f^n_{ib} = C^n_b f^b_{ib} \tag{1.17}$$

The first step of the process is to update the attitude using the current data in order to obtain the current attitude orientation. By knowing the previous attitude it can be demonstrated [1] that the translation to an ENU frame is:

$$C^n_b(+) = C^n_b)(-)(I_3 + \omega^b_{ib}\tau) - (\omega^n_{ie}(-) + \omega^n_{en}(-))C^n_b(-)\tau \tag{1.18}$$

Where :

- C^n_b is the attitude matrix.
- Index $(+)$ and $(-)$ represent the current and previous estimations.
- ω^n_{ie} is the Earth-rotation rate.
- ω^n_{en} is the ENU rotation or transport-rate.
- τ is the time step since the last iteration.

Once the attitude has been computed, the accelerometer data can be transformed into a force-specific frame using 1.17. Specific force can then be integrated in order to obtain a velocity v^n_{eb} solution in an ENU frame:

$$v^n_{eb}(+) = v^n_{eb}(-) + [f^n_{ib} - (\omega^n_{ie}(-) + \omega^n_{en})v^n_{eb}(-) + g^n_b]\tau \tag{1.19}$$

Where a new term g^n_b is included to compensate for local gravitational differences and Coriolis force. An additional integration can then be done in order to obtain a position solution r^e_{eb}:

$$r^e_{eb}(+) = r^e_{eb}(-) + \frac{\tau}{2}(v^n_{eb}(-) + v^n_{eb}(+)) \tag{1.20}$$

The output of the INS propagation in an ENU frame can then be converted easily to ECEF frame, which is more convenient for GNSS integration.

CHAPTER 2. KALMAN FILTER

The Kalman filter is an estimation algorithm that allows estimating the correct value of a set of parameters (called states) in noisy environments. It takes advantage of known properties of the system (such that the integral of speed becomes the position) to compute an estimate of the state. This estimate can then be mixed with a new measurement using a weighted factor called the Kalman Gain. The Kalman gain uses the covariance of the measurements and the states to determine which one is more accurate. This technique allows accurate readings even in noisy environments and it is widely used in navigation.

In the next sections we will present the equations and steps of the Kalman Fitler and how it is initialized. [1]

2.1. Equations

2.1.1. State Propagation

In order to study the functioning of a Kalman filter, let us see it in a positioning case. Figure 2.1.1. shows an overview of the entire algorithm and the different interactions of the variables.

For GNSS positioning, the wanted output is position, velocity and time offset of the receiver clock, what is commonly known as a Position Velocity Time (PVT) solution. These values are called states (our unknowns) and they are placed inside the state vector $\hat{X}$.

$$\hat{X} = (x, y, z, \dot{x}, \dot{y}, \dot{z}, \delta t, \delta \dot{t}) \tag{2.1}$$

Where:

- x, y, z Are the position coordinates.
- $\dot{x}, \dot{y}, \dot{z}$ Are the Cartesian velocity components.
- $\delta t, \delta \dot{t}$ Are the receiver clock bias and drift explained in Section 1.2.2. .

A number of additional parameters allow us to describe the accuracy of the state vector and how it changes over time:

- Propagation matrix ϕ. This matrix defines how the state vector $\hat{X}$ changes from one iteration to the next. For example position is the integral of speed.
- Error covariance matrix P, which defines the deviation of the state and how the errors of one state translate to another.
- System covariance matrix Q, which includes information on noise introduced by the system over time.

Once this parameters have been introduced, the states can be propagated from one iteration to the next using the following formulas:

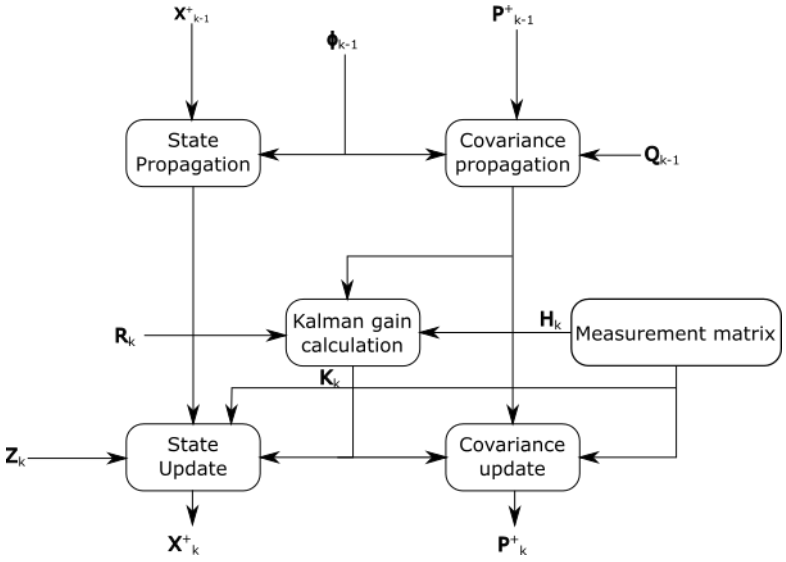

Figure 2.1: Overview of the Kalman Filter variables

$$\hat{x}_k^- = \phi_k \hat{x}_{k-1}^+ \tag{2.2}$$

$$P_{k|k-1} = \phi_k P_{k-1}^- \phi_k^T + Q_k \tag{2.3}$$

2.1.2. Measurement Update

The propagated terms do not add any new information. In order to account for new changes, the Kalman filter also adds new measurements in parallel to the propagation. The measurements are defined by:

$$\delta z_k^- = z_k - H_k \hat{x}_k^- \tag{2.4}$$

Where Z_k is he measurement vector in the current iteration (a vector including the pseudorange and pseudorange rate measurements from all satellites). H_k is the measurement matrix defined in Section 1.2.3..

As with the states, a measurement covariance matrix R can be defined, including information on the accuracy of the measurements. This matrix is defined by the Kalman filter designer, and it will be used to know how much new measurement must be trusted in comparison to the state propagation. More information on the measurement covariance matrix is explained in Section 5.

2.1.3. Kalman Gain

Up to this point then, the algorithm has computed a prediction of the states, and a measurement update. The measurements are prone to noise, while the prediction does not incorporate any new information, it just propagates old data. Both can be incorporated in an averaged mean called Kalman Gain. What the Kalman Gain does is average prediction and measurements using their covariance matrices to weight each one. The formula of the Kalman gain is:

$$K_k = P_k^- H_k^T (H_k P_k^- H_k^T + R_k)^{-1} \tag{2.5}$$

The Kalman gain K can then be used to merge both the measurements and the state propagation. Each state will be updated depending on the weighting of the computed Kalman gain. The updated state vector $\hat{x}_k^+$ and covariance matrix P_k^+ can then be used on the next iteration

$$\hat{x}_k^+ = \hat{x}_k^- + K_k \delta z_k^- \tag{2.6}$$

$$P_k^+ = (I - K_k H_k) P_k^- \tag{2.7}$$

Chapter 3 will further expand the explanation on the Kalman filter for the specific case of GNSS and INS integration.

2.2. Initialization

As said earlier the Kalman filter requires information of the previous iteration in order to work. The first iteration therefore cannot be done in the Kalman filter, but rather it relies in another method, like the Least Square Error (Equation 1.16) in order to obtain a valid solution. The output of the WLSE solution will be used as the initial point for the Kalman filter. It must initialize the state vector and also the covariance matrix P.

As both the state vector and the covariance matrix are updated at every iteration using new measurements initialization values do not need to be extremely accurate, as their effect is quite limited.

CHAPTER 3. STATE OF THE ART

The following section will describe the state of the positioning algorithm used for positioning and the hardware used for the tests and trials.

The positioning algorithm expands on the concepts explained in Chapter 2 and merges the equations showed in Sections 1.2. and 1.5..

3.1. Integration Kalman Filter

In Section 2 we have talked about the Kalman filter using only measurements from GNSS: Pseudorange and Doppler frequency. The Filter takes these two values and merges them to generate an accurate estimate of the user's position and velocity. More data can be mixed together with the GNSS measurements in order to obtain a much more precise output.

Stand-alone GNSS solutions offers a good absolute position and velocity solution, with a relatively poor update rate (generally 1 Hz), no attitude information and it suffers from outages in urban canyons. INS on the other hand can offer a high update rate (100 Hz), attitude information and it can work continuously, yet they suffer heavily from drift. It makes sense then to combine them together to mix the pros and eliminate the cons.

Integration of both sensors can be done at different levels. Literature [1] [4] describes the following types:

- **Loosely coupled integration:** In this type the GNSS and INS positions are computed separately and then mixed together to obtain an average. This method is simple and offers redundancy, yet it can only work if four satellites are visible for the GNSS solution.
- **Tightly coupled:** In which the INS solution is mixed with the raw pseudoranges and Doppler measurements. This system works well for low coverage areas like urban canyons as it can work with less than four satellites. The disadvantage is that a receiver capable of outputting raw data is necessary.
- **Deeply coupled:** Where the receiver digital output is mixed in the Kalman filter, an the output is used to control more accurately the receivers tracking loops. This type of receiver requires a software receiver in order to be implemented.

Tightly coupled is the algorithm structure used, as it offers the best compromise: It is more simple to implement than deeply coupled yet it is far more effective than loosely coupled for urban environments. The overview of the algorithm can be seen in Figure 3.1.. An INS Position, velocity and attitude (PVA) solution is computed constantly by the INS. Once GNSS measurements are available they are mixed with the INS. The integration produces a position, velocity, time and attitude solution (PVTA) and an estimation of the IMU biases. The biases can be fed back to the INS to perform a calibration.

Following is a more accurate description of the algorithm and the mathematical formulas behind it.

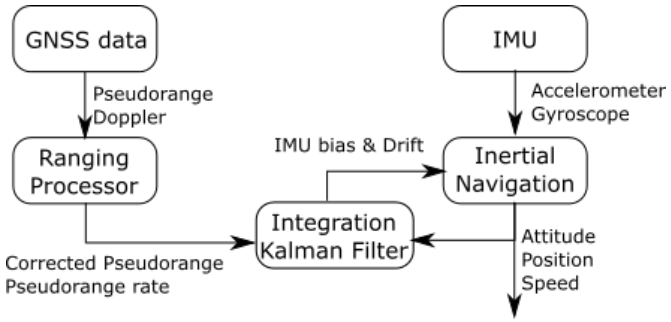

Figure 3.1: Structure of a tightly coupled integration using Kalman filter

3.1.1. State Vector

Chapter 2 introduced the Kalman state vector for a GNSS only solution. To accomodate for the new number of variables (seventeen in total), the state vector for INS/GNSS integration becomes:

$$\hat{x} = (\Phi, v, r, b_F, b_\Omega, \delta t, \delta \dot{t}) \tag{3.1}$$

Where:

- Φ is the vehicle attitude (Pitch, roll and heading)
- v is the user speed.
- r is the user position.
- b_a is the accelerometer bias.
- b_g is the gyroscope bias.
- δt is the user clock bias.
- $\delta \dot{t}$ is the user clock drift.

In order to accommodate the new variables, the transition matrix ϕ, the state covariance matrix P and the system covariance matrix Q must be adapted. The measurement matrix H and measurement covariance matrix R will remain the same as in equation 1.16, as they are dependent on the number of GNSS measurements, not on any INS parameter.

3.1.2. Transition Matrix

It can be demonstrated [6] that the transition matrix ϕ becomes:

$$\phi = \begin{pmatrix} I_3 - \Omega_i^e e\tau & 0_3 & 0_3 & 0_3 & C_e^b\tau & 0_{3,1} & 0_{3,1} \\ -(C_e^b f_i^b b)\tau & I_3 - 2\Omega_i^e e\tau & g_e\tau & C_e^b\tau & 0_3 & 0_{3,1} & 0_{3,1} \\ I_3 & I_3\tau & I_3 & 0_3 & 0_3 & 0_{3,1} & 0_{3,1} \\ 0_3 & 0_3 & 0_3 & I_3 p_m & 0_3 & 0_{3,1} & 0_{3,1} \\ 0_3 & 0_3 & 0_3 & 0_3 & I_3 p_m & 0_{3,1} & 0_{3,1} \\ 0_3 & 0_3 & 0_3 & 0_3 & 0_3 & 1 & \tau \\ 0_3 & 0_3 & 0_3 & 0_3 & 0_3 & 0 & 1 \end{pmatrix} \tag{3.2}$$

Where

- I_3 is a $3x3$ identity matrix.
- $\Omega_i^e e$ is the earth rotation correction described in 1.5.2..
- C_e^b is the rotation matrix from body reference to ECEF.
- p_m is the propagation factor in a Gauss-Markov process [1].
- τ is the time step from the previous iteration.

3.1.3. System Covariance Matrix

The system covariance matrix Q can also be defined very easily [1] as:

$$Q = \begin{pmatrix} S_g & 0 & \cdots & \cdots & \cdots & \cdots & 0 \\ 0 & S_a & 0 & \cdots & \cdots & \cdots & 0 \\ 0 & 0 & 0 & \cdots & \cdots & \cdots & 0 \\ 0 & 0 & 0 & S_{ba} I_3 & \cdots & \cdots & 0 \\ 0 & \cdots & \cdots & 0 & S_{bg} I_3 & 0 & 0 \\ 0 & \cdots & \cdots & \cdots & 0 & S_c & 0 \\ 0 & \cdots & \cdots & \cdots & \cdots & 0 & S_c d \end{pmatrix} \tag{3.3}$$

Where the parameters S_g, S_a, S_{ba}, S_{bg}, S_c and $S_c d$ are respectively the gyroscope, accelerometer, gyroscope bias, accelerometer bias, clock and clock drift power spectral densities functions (PSDs).

3.2. Hardware

This section will introduce the hardware used for the test cases and the integration on the reference vehicle.

Different types of receivers were used in order to perform the tests required. The initial hardware used consisted of a U-blox LEA-6T [18] receiver combined with an tactical grade IMU from XSens [19]. The xSens MTi was the cheapest navigation capable IMU available. Figure 3.2. shows the mounting of all the equipment in a van right before a test.

This type of configuration represented the cheapest possible INS/GNSS integration. As a reference a Novatel receiver was used. It is a dual frequency, GPS and GLONASS

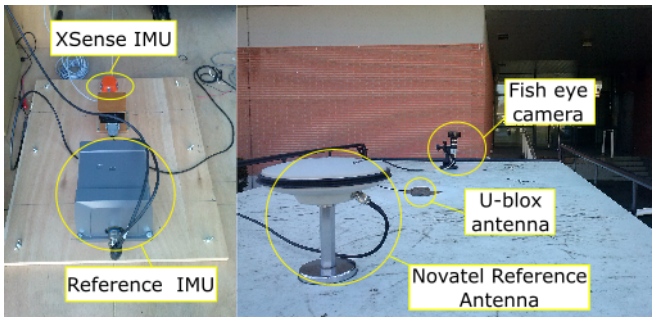

Figure 3.2: Harware mounting on the van

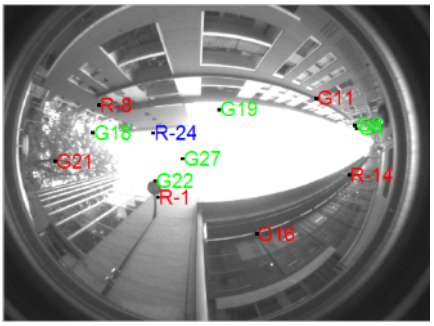

Figure 3.3: Camera discrimination

receiver combined with a Novatel SPAN IMU [20]. Overall, centimeter level accuracy, even in urban canyons, can be achieved. The reference path can then be used to compute the accuracy of the integrated solution. It is worth mentioning that both the Novatel and U-Blox measurements are synchronized by GPS time with an accuracy of the order of nanoseconds[21]. The xSense was also synchronized to GPS time trough the U-Blox. As the LEA-6T is a timing module, it can accurately timemark each of the IMU measurements.

In order to also use GLONASS measurements, at first the Novatel reference data was used. In order to simulate the behaviour of a cheaper receiver, only single frequency measurements were used, and they were integrated together with the XSense IMU in order to offer a much more accurate simulation of a cheap receiver. It was seen however that this configuration was not a correct representation of the performance of a cheaper receiver, as the Novatel receiver antenna filters much of the multipath satellites.

For the final test of the full algorithm, a Furuno VN-870 [23] receiver was supossed to be used. This receiver was a low cost multi GNSS receiver, capable of GPS, GLONASS and SBAS measurements. Unfortunately, this receiver could not be used for the thesis.

In order to increase the accuracy of the U-Blox receiver, a fish eye camera [22] was mounted on the top of the vehicle as seen in Figure 3.2.. Its purpose was to detect surrounding buildings and differentiate them from the visible sky area. This algorithm allowed to filter out those satellite that were not in direct Line of Sight. The objective is to limit NLOS signal effect as explained in section 1.3.1.. Figure 3.2. shows a snapshot on how the camera works by filtering out NLOS satellites (indicated in red).

A more extended explanation on this algorithm can be found in [6]

CHAPTER 4. IMPLEMENTATION

This section will cover the main changes done to the positioning algorithm in order to increase its accuracy in urban areas. This changes include

- **MultiConstellation implementation:** Implementation of GLONASS.
- **Carrier-to-Noise density models and masking:** Weighting of the measurements in the Kalman Filter.
- **GNSS/INS lever arm compensation:** Compensate for the position difference between GNSS and INS solutions.

4.1. Multi Constellation Implementation

As explained in section 1.4.1., the advantages of having two constellations are a much higher availability in zones with limited visibility like urban canyons. The main expected effect of the multi constellation implementation were:

- **Increased accuracy:** as areas with less than four satellites get reduced, visibility in urban areas can increase almost up to the level of clear sky and thus he accuracy.
- **Reduced heading drift:** a higher number of satellites can correct the high IMU bias present in the solution. The estimation of these bias inside the Kalman filter (Section 3.1.1.) can then be fed back to the INS propagation, reducing furthermore the error, especially the yaw's.

4.1.1. GLONASS Implementation

As the second most numerous GNSS constellation, GLONASS was the highest priority to be implemented in the algorithm. It is also, due to historical reasons, the most difficult one to be integrated with GPS, as compatibility was never a consideration during the design stage.

Remembering the main differences explained in 1.4.3. we find that the algorithm must account for the following aspects:

- **Time reference**
- **Ephemeris and satellite position calculation**
- **Signal frequency**
- **Solution Accuracy**

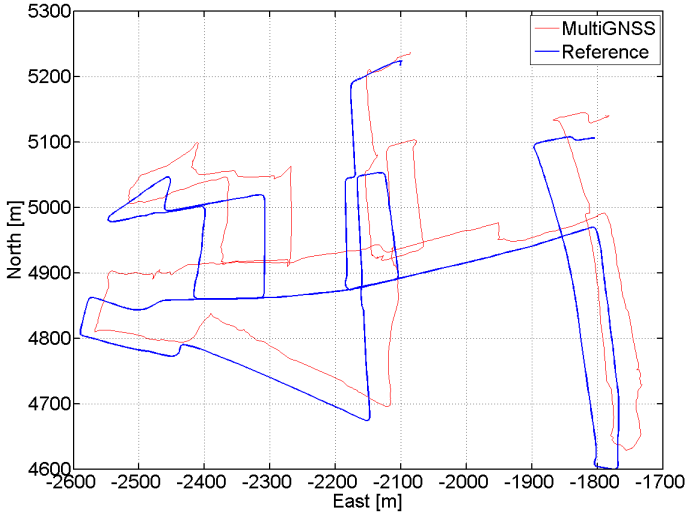

Figure 4.1: Combined GPS and GLONASS solution without compensating for the different time references.

4.1.1.1. Time reference

GLONASS time is defined by the Russian reference of UTC known as UTC (SU)[10]. Its difference with GPS (GPST or UTC(USNO)) time consists of a number of integer seconds (known as leap seconds) that UTC has corrected since the start of GPST in 1981 plus an unknown number of delay that is not measured by neither of the ground segments and that is not transmitted in their respective navigation messages.

To accomodate for this difference, the integration Kalman filter described in Section 3.1.1. must be modified to accommodate a new clock bias estimation $\delta t_{GLONASS}$ and clock drift $\delta i_{GLONASS}$. The state vector described in Equation 3.1 thus becomes:

$$\hat{x} = (\Phi, v, r, b_F, b_\Omega, \delta t_{GPS}, \delta i_{GPS}, \delta t_{GLONASS}, \delta i_{GLONASS}) \tag{4.1}$$

Figure 4.1.1.1. shows the effect of not taking into account this new compensation. It shows a GPS and GLONASS (no INS) in which GPS clock bias estimation has been applied to GLONASS measurements. The leap seconds have been corrected for, otherwise the error is too high to even obtain a solution.

4.1.1.2. Ephemeris calculation

GLONASS ephemeris contain different information than GPS's. GLONASS transmits its orbital parameters in raw Cartesian format. Acceleration and speed must be integrated over the desired time interval in order to obtain the satellite's position at transmission time. GLONASS Interface Control Document [10] describes an algorithm to perform orbit integration, achieving sub-meter accuracy [24].

The other difference in the ephemeris is the definition of the relativistic effect and satellite clock corrections. In GPS, these two corrections are transmitted in different values, while in GLONASS they the relativistic effects are transmitted inside the satellite clock error.

The result of these differences is that the orbital integration of GLONASS satellites has to be done differently than GPS, increasing the complexity of the algorithm and the necessary computing power.

4.1.1.3. Signal frequency

GLONASS L1 band (Also called G1) had a center frequency of 1602 MHz and it spans between 1593 MHz to 1610 MHz. Due to the FDMA nature of GLONASS, the bandwidth is very wide, as each satellite much be assigned a different frequency channel in the spectrum. The frequency number k of each satellite is transmitted in the ephemeris, and the center frequency of each satellite can be computed using the equations[25]:

$$F_1(k) = 1602 + k * 9/16MHz \tag{4.2}$$

$$F_2(k) = 1246 + k * 7/16MHz \tag{4.3}$$

$F_1(k)$ and $F_2(k)$ being the central transmitting frequencies of satellite k for the G1 and G2 bands as defined in Section 1.4.3..

This frequency differences creates a few particularities to GLONASS receivers. For the hardware part, GLONASS receivers must use a GLONASS antenna, as a normal GPS antenna will filter out other bands outside GPS L1. In the algorithm, it means that any frequency dependant component must be adapted.

For example, the computation of the pseudorange rate using Doppler shift measurements explained in Section 1.2.4. needs to be adapted to the new GLONASS frequencies. A difference of only $30Hz$ in the Doppler shift can cause a difference of up to $100\ \frac{km}{h}$ in the instantaneous speed estimation depending on the satellite-user relative speed. The difference between GLONASS and GPS frequencies is more than 30 MHz, so the frequency must be taken into account.

The last frequency dependent term is the ionospheric correction. The delay caused by the ionosphere depend on the carrier frequency. It is worth noting that GLONASS does not have ionospheric model and hence transmits no corrections in its ephemeris. GPS Klobuchar model however can be used by applying a frequency correction[26]

$$Iono_{factor} = \frac{f_{L1}}{f_{G1}} \tag{4.4}$$

4.1.1.4. Solution accuracy

Other differences with GPS mildly affect the accuracy of GLONASS. The shorter transmission rate (called chip rate)and transmitted power makes tracking less accurate, making them not as valuable as GPS satellites [11]. For high accuracy solutions, the datum difference should also be taken into account. To compensate for this reduction on the solution quality, GLONASS measurements should be down weighted with respect to GPS in the Kalman filter. Further explanation of this topic can be found in Section 4.4., while the testing is in Section 5.2.1..

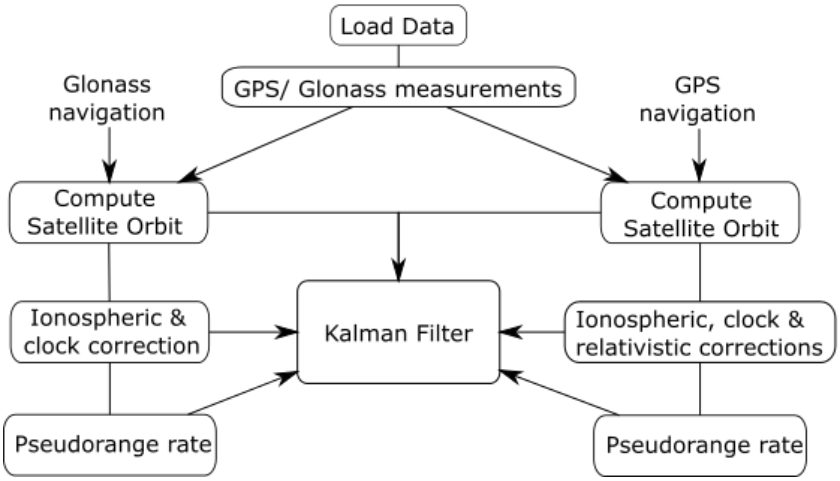

Figure 4.2: Overview of the multi constellation algorithm

4.1.1.5. Algorithm overview

The result of all these difference is that GPS and GLONASS measurements must be processed differently before the Kalman filter as information is not on the same reference, which causes additional complexity to the algorithm, specially when compared to more modernized systems like Galileo and Beidou.

Taking all the mentioned parameters into account, a comprehensible vision of the algorithm can be seen in Figure 4.1.1.5.. Observables come mixed in a RINEX[27] format file. Satellites must then be divided in order to perform the different computations separately. Once all the corrections have been calculated, measurements can be mixed and applied to the Kalman Filter. The only difference inside the filter are the addition of the GLONASS clock bias and drift as described in 4.1.1.1..

4.1.2. Galileo and Beidou

Other constellations are easier to adapt and integrate with GPS measurements than GLONASS. As explained earlier in Section 1.4.4. Galileo and Beidou were already developed with integration in mind. Since the different system time differences are already included in the respective navigation messages, no additional states are required in the Kalman filter, therefore adding no additional computing complexity. Also they use the same orbit determination algorithms as GPS. Figure 4.1.2. shows all constellations integrated. Galileo and Beidou processing goes parallel to GPS.

Unfortunately, by the time of the writing no multiconstellation receiver was available and Galileo and Beidou integration could not be fully implemented.

4.2. Carrier-to-Noise Density Models And Masking

GNSS satellites are placed at Medium Earth Orbit, at some 20.000 Km from the surface of the Earth. Radio signals must cross this vast empty space, the Earth's ionosphere and

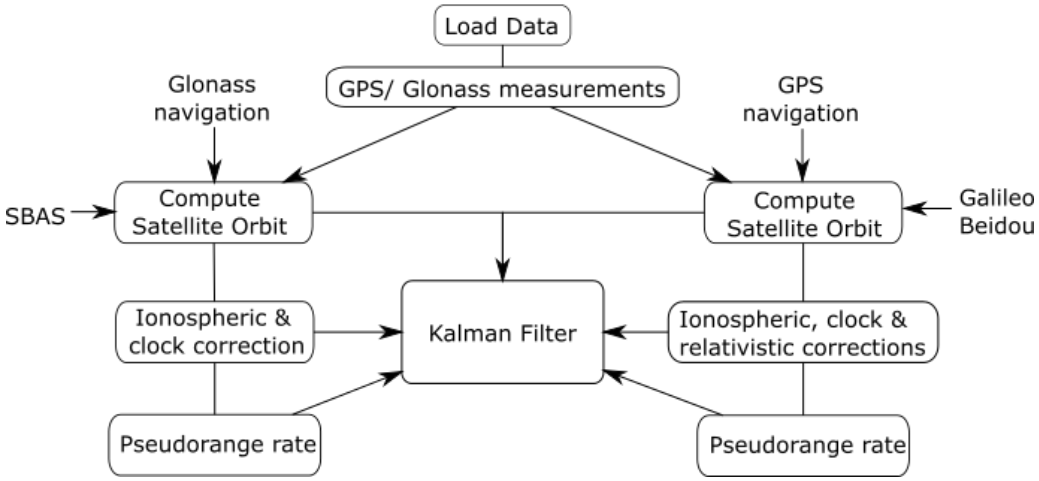

Figure 4.3: Modified algorithm for all constellations

troposphere before reaching a receiver on the surface. The power of the GPS L1 C/A signal is 25 W, which is then amplified by a factor of 13 dBi by the satellite's antenna, making a total transmitted power of 500W or 27 dBW (Less power than a kitchen oven). Power then decreases with distance by a squared factor. For a distance of 20000 Km the power looses are some 182 dBW, giving a received power of -155 dBW (or $3.16 * 10^{-16}$ W). This is an insignificant amount of power, well below the termal noise of the environment.

Once demodulated, the GPS receiver is capable of computing the carrier-to-noise density. This ratio, called C/N_0, refers to the comparison between the received power of the signal compared to the noise level of the environment. The theoretical output of this equation can be seen on Equation 4.5 [29].

$$C/N_0[dBHz] = P_r + G_r - 10\log_{10}(k) - 10\log_{10}(T_{sys}) - L \tag{4.5}$$

Where:

- C/N_0 is the carrier-to-noise density.
- P_r is the received power.
- G_r is the receiver antenna gain. It changes with the satellite elevation.
- k Boltzman's constant $1.38 * 10^{-23} J/K$
- T_{sys} System temperature.
- L System loses (2dB).

C/N_0 measurements are generated by the receiver for all satellites, and it indicates how strong the arriving signals are. Typical C/N_0 values will be:

- $35 - 50$ dBHz for LOS satellites
- $20 - 35$ dBHz for NLOS satellites.

In the following section we will talk on how these measurement have been used in the computation of a navigation solution in the Kalman Filter. In particular we will talk:

- How the measurement have been used to weight down inaccurate satellites and the different models applied.
- How the measurement have been used to discard satellites entirely from computation(mask).

4.2.1. Relationship Between Carrier-to-Noise Density And Position Accuracy

In Section 2 we talked about the measurement covariance matrix R used in the Kalman filter to quantify the errors present in all measurements. This matrix will be used to weight down noisy measurements in order to take them less into account for the computations of the PVTA solution. In this section we are going to enter deeply into how the values for this matrix can be found using C/N_0 values for the modelling.

As explained earlier in Section 4.2. C/N_0 indicates how powerful the received signal is, compared to the noise level of the environment. Higher C/N_0 values will make the signal easier to track, reducing the noise of the tracking loops, making them more accurate and obtaining overall better accuracy results. A relationship can be seen between C/N_0 values and position accuracy.

Carrier-to-noise density can be reduced by two factors: either the received power is reduced, or the noise floor is increased. The noise floor can be increased by an increase in temperature (T_{sys} in Equation 4.5) or by any other additional signal in the band. When GNSS signals get demodulated and correlated using PRN codes, only the original, desired signal is obtained. Any additional signal on the band (from other satellites, constellation or from multipath) will be turned into noise after the correlation [30].

On the other hand, C/N_0 can be reduced by the reduction of received power. The main reasons being:

- Blocking: Signal gets partially blocked by buildings, trees or water vapour in the air. Any additional obstacle along the way of the signal will further reduce its power level.
- Elevation: Satellites in lower elevation have to cross more atmosphere than zenith satellites. A direct relationship exist between C/N_0 and elevation.

If a relationship between C/N_0 and visible satellites can be made, blocked satellites can be down weighted or excluded from the computation, reducing the effects of multipath in the solution. If too many satellites are excluded however, the solution will degrade due to the lack of visibility. Therefore it is more important to have as many satellite visible as possible, and the need for a multi constellation receiver is even more important when satellites are being excluded.

4.2.2. Weighting Of Measurements

The relationship between C/N_0 and position accuracy must be made using an statistical model that tries to represent this relationship. This model can then be included in the measurement covariance matrix R described both for the WLSE solution in Equation 1.16 and in the Kalman filter equation seen in Section 2.1.. This covariance matrix is defined as:

$$R = \begin{pmatrix} \sigma_{z_1}^2 & 0 & 0 & 0 \\ 0 & \sigma_{z_2}^2 & 0 & 0 \\ \vdots & \vdots & \ddots & \vdots \\ 0 & 0 & 0 & \sigma_{z_n}^2 \end{pmatrix} \tag{4.6}$$

Where $\sigma_{z_n}^2$ is the covariance of each of the different satellites n seen by the receiver. For the positioning algorithms defined in 1.16, where only pseudorange and Dopper shift measurements are taken from each satellite (Carrier phase measurements are not included in the algorithm), covariance matrix R can then be defined as:

$$R_{2nx2n} = diag(\sigma_{PR_1}, \cdots, \sigma_{PR_n}, \sigma_{D_1}, \cdots, \sigma_{D_n}) \tag{4.7}$$

Where :

- n is the number of used satellites.
- R is the covariance matrix of size $[2n, 2n]$, where the diagonal components are the covariances and the off-diagonal components are zero.
- σ_{PR_i} is the covariance of the pseudorange measurement for satellite i.
- σ_{D_i} is the covariance of the Doppler shift measurement for satellite i

The following section will describe the different models used for the computation of both σ_{PR_i} and σ_{D_i}. This models are just introduced and will be tested in Chapter 5.

4.2.3. Existing Models

4.2.3.1. Elevation based model

The model that was currently implemented in the Kalman filter for the computation of the measurement covariance matrix was based on satellite elevation. That is, the covariance of the pseudorange measurements was a function of elevation. A simplified version of the algorithm is:

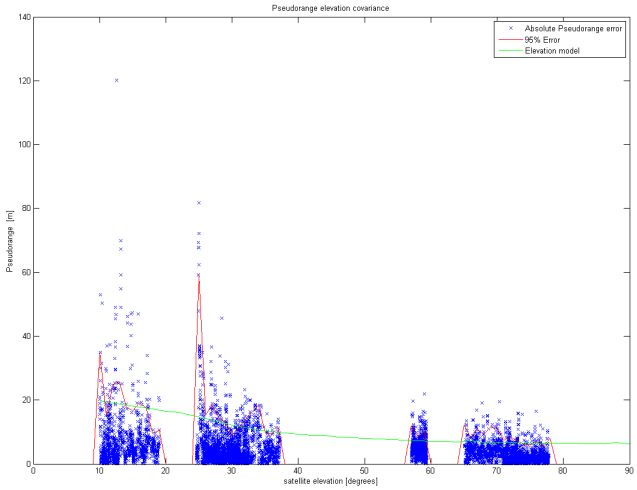

Figure 4.4: Fitting of the elevation model into a pseudorange over C/N_0 data set.

$$\begin{aligned} \sigma_{ionosphere} &= f(\theta,\phi) \\ \sigma_{troposphere} &= f(\phi) \\ \sigma_{receivernoise} &= 1.5m \\ \sigma_{multipath} &= f(\theta,e) \end{aligned} \tag{4.8}$$

Where:

- σ is the standard deviation in the pseudorange measurements.
- θ is the satellite elevation.
- ϕ is the receiver's latitude.
- e is an environmental constant set by the designer: $e = 3$ for urban environments

The total User Equivalent Range Error $UERE$ for each satellite sat can be found using Equation 4.9

$$UERE_{sat} = \sqrt{\sigma^2_{ionosphere} + \sigma^2_{troposphere} + \sigma^2_{receivernoise} + \sigma^2_{multipath}} \tag{4.9}$$

The statistical fit of this model into the collected data set can be seen in Figure 4.2.3.1. , which represent the change of pseudorange error over satellite elevation. The 95% value is painted in red, while the standard deviation σ is in black. Ideally, the model should fit the σ curve in order to obtain the best possible estimation of the covariance.

4.2.3.2. Problems

Early result showed that this model was not well suited for modelling of error in urban areas as it did not down weight enough blocked satellites. The biggest source of errors in urban areas is multipath caused by NLOS satellites, a model based on elevation will

Figure 4.5: Difference in carrier-to-noise values between LOS (green) and NLOS (red))

not be able to discriminate and weight down satellites, as a high elevation satellite could be blocked. This information pushed the search for a better model that could effectively weight down blocked satellites to increase the accuracy in urban areas. C/N_0 models will be more effective as there is a much clearer relationship between carrier-to-noise density and LOS satellites.

4.2.3.3. Pseudorange rate model

A different model is applied to Doppler measurements. The applied model is table based, and it changes as a function on both carrier-to-noise density and user speed. The look-up table can be found in [11] and it was developed for heavily degraded environment. This model was well suited for urban environments, as it was designed in those circumstances.

4.2.4. New Carrier-To-Noise Density Based Models

Error models based on C/N_0 will offer a better approximation to distinguish between visible and blocked satellites. Figure 4.2.4. shows the distribution of data from a U-Blox LEA-6T receiver in an urban environment. Green represent LOS and red NLOS where the camera described in Section 3.2. is used to discriminate between both. In the graph it can be seen that C/N_0 values above 40 dBHz can be considered as LOS. Values below 30 dB-Hz are considered as from NLOS satellites. Errors seem to persist in the graph from NLOS satellites at high C/N_0 values and viceversa. This fact is assumed to be caused by errors in the camera as sometimes clouds can be detected as building [6].

4.2.4.1. Pseudorange model

The tested pseudorange model was obtained from [31]. It was obtained in an urban environment, and therefore should adapt well to the multipath circumstances in Toulouse. The model is based on an empirical model and it is defined as:

$$\sigma_P^2 = a + b \cdot 10^{\frac{-C/N_0}{10}} \tag{4.10}$$

Table 4.1: Variables for Equation 4.10 depending on the environment

Environment	a	b
City [11]	-1.5	731^2
Heavily Degraded pseudorange rate [31]	0.001	40

Where σ_P^2 is the covariance value for the pseudorange measurements referenced in Equation 4.7. parameter a and b are dependent on the type of environment. Table 4.1 shows the different types of values used in the different environments.

4.3. Satellite Masking

So far we have talked about weighting of values used for the R matrix in order to weight down noisier satellites for the PVTA computation. Masking consists of setting a threshold and setting a high weighting factor for any satellite with a lower CNR. This eliminates the satellite from the computation. It acts more strongly than weighting in the sense that it is ensured that the satellite will not be used.

4.3.1. Carrier-to-Noise Density Mask

Figure 4.2.4. already gave a clue of the concept behind masking. It can be seen that some boundary must exist between 30 and 40 $dBHz$ which sets the difference between LOS and NLOS. In order to find this boundary, repetitive test were done on a urban data set.

The implementation of the mask is done through imposing a high weighting factor for the satellite in the covariance matrix R. Remembering Equation 2.5, the Kalman gain computes a weighted average between the state prediction and the measurements using their covariance matrices, R and P. A heavy weighting factor will put more importance on the other satellites or on the state prediction (if it is the only satellite available) ensuring it will not be used.

4.3.2. Different Pseudorange And Doppler Mask

Signal reflection affects the travel time, power and frequency of the transmitted signal. The masking applied so far assumed that both pseudorange and Doppler measurement were affected the same way by multipath. So any signal whose power is below a threshold is considered to have unusable pseudorange and Doppler measurements.

This might not be the case, as the nature of the reflection might be different for pseudorange and carrier frequency. It is then worth trying whether different masking threshold can be applied to Doppler and pseudorange measurements. The masking is applied as described in 4.3.1. rather than fully deleting the satellite from the computation. This makes the implementation of the masking scheme between Doppler and pseudorange easier .

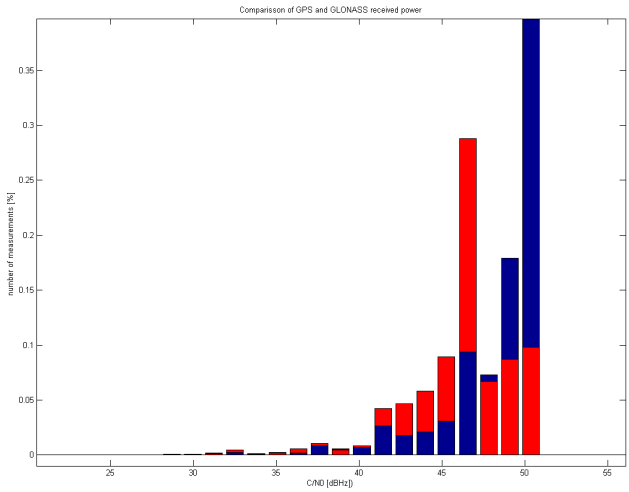

Figure 4.6: Difference in received power between GPS (blue) and GLONASS (red)

4.4. Considerations For GLONASS

In section 4.1.1.4. we introduced the weighting of GLONASS measurements with respect to GPS due to the lowest quality of its measurements. Authors[24] have defined this weighting as bad as a factor by 3, although it has improved in recent years. Tests where conducted with the Novatel receiver, post processing the tests runs by different factor.

4.4.1. Masking

In Section 4.3. we discussed the effects of masking based on the carrier-to-noise density. As explained in Section 1.4.3. GLONASS has a lower received power than GPS, therefore any C/N_0 masking will always be excessive. This difference in the transmitted power can be seen in Figure 4.4.1., where one can see a histogram of GPS and GLONASS measurements normalized by the number of measurements of each constellation. It can be seen that GPS does have a higher received power. GLONASS measurements where found to be 2 dBHz less powerful than GPS's for a satelllite in the same elevation and visibility. Hence a new threshold for GLONASS should be set.

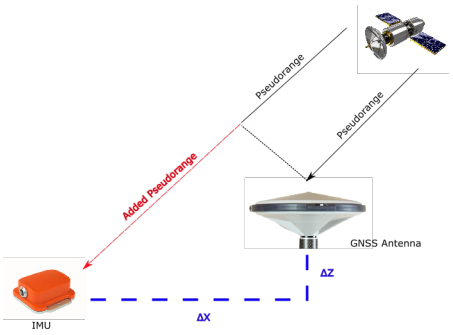

Figure 4.7: Effects of the Lever Arm

4.5. Lever Arm

In Section 3.1. we described the integration of INS and GNSS measurements. In that case, both INS and GNSS solutions where considered to have the same center, where in reality they both compute a position solution around a difference place. INS computes position of the IMU, while GNSS measures position at the antenna phase center. Figure 4.5. shows the difference between both in a 2D example. The real distances measured where 1.7 m for the vertical elver arm and 0.3 m for the horizontal. This distances were also tested iteratively in the algorithm, and they correspond to the smallest error.

The IMU position is then moved before the Kalman filter, where the integration takes place, in order to compensate for this distance, as it affects both the pseudorange and Doppler. Lever arm accounted for a small increase in position and yaw accuracy, yet not big enough to compensate the big yaw errors present in the solution.

CHAPTER 5. TEST

This chapter will present the different results obtained from post processing two data sets. These were captured using the same layout as the one described in Section 3.2.. It is worth mentioning that for this results it was planned that they would be captured using a low cost, multi constellation Furuno receiver. Yet at the point of the writing such a receiver was not available. Instead, data from the U-Blox receiver was used together with the GLONASS data of the Novatel reference receiver. Only L1 data was used, simulating the performance of a mass market receiver.

This chapter will be structured as follows. First, the test scenarios from which data was gathered will be introduced. Following will come the evaluation of the different models and masking threasholds introduced in . The results will be evaluated at the end.

5.1. Test Cases

Three different tests cases were used. The first one was an all urban test taken in Toulouse center during October 2014. This data set includes some twenty minutes of data. The second and third one were taken on the same day in February 2015. One data set was taken in the morning and the other in the afternoon and lasted some forty minutes each. The objective was to obtain a higher distribution in the elevation of satellites. Figure 5.1 shows the three different routes. The October run (in green) shows a full urban environment. The blue route corresponds to the morning run in February 2015, while the red one corresponds to the one taken in the afternoon. Between them we obtain a very good combination of all the types of urban environments present in Toulouse: Closed urban in the city center and more open suburban environments in the outskirts.

5.1.1. Evaluation Of Performance

Performance of each of the different models will be evaluated based on their horizontal and yaw accuracy. These parameters will be considered the main ones, as they offer the simplest, quickest evaluation method for each weighting scheme. Of these two measurements, the root mean square , 95% deviation and maximum error will be the parameters used for comparison.

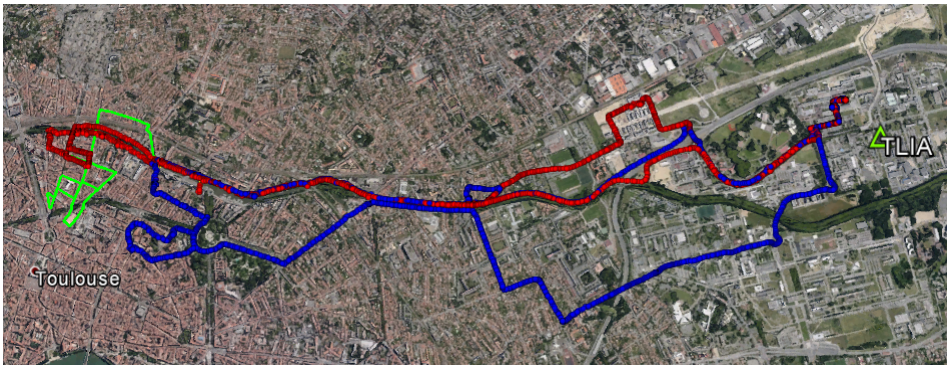

Figure 5.1: The three different routes for the measurement campaigns

Initially all variables were monitored. Eventually it was seen that pitch and roll tended not be affected by any configuration and their values always remained very low. They were only monitored during debbuging, as they will have huge errors in case of a programming mistake (such as inverting the axis of the IMU). Vertical error is always a problem when using GPS, as it tends to be twice as large as the horizontal. As the models are only for land applications, the vertical error is not considered.

5.2. Weighting Models

In Section 4.2.2. we introduced the different weighting schemes used in order to compute the measurement covariance matrix R. This models are developed and tested for different environments, and so it was requested to test their performance in the urban environment of Toulouse.

The fully urban environment presented the most challenging. As explained in earlier sections, multipath has the biggest effect due to buildings and satellite visibility is at its lowest. The weighting of satellites must control this balance, punishing heavily those satellites that are susceptible to multipath (with low carrier-to-noise density). Table 5.1 shows the accuracy results for urban environment using the U-Blox receiver only and the models described in 4.2.2..

Table 5.1: Comparison of models performance in Urban environment for the U-Blox (no camera)

	Old models	New pseudorange model	New pseudorange and Doppler models
Horizontal RMSE [m]	14.80	9.88	8.21
Horizontal error 95% [m]	27.79	20.55	15.62
Horizontal error maximum [m]	39.06	38.82	24.39
Yaw RMSE [°]	20.57	20.39	13.56
Yaw error 95% [°]	27.13	27.32	21.46
Yaw error maximum [°]	104.33	95.79	26.79

Table 5.2: Comparison of models performance in suburban environment for the U-Blox (no camera)

	Old models	New pseudorange model	New pseudorange and Doppler models
Horizontal RMSE [m]	6.84	6.15	6.09
Horizontal error 95% [m]	16.57	12.40	11.66
Horizontal error maximum [m]	29.68	21.73	22.35
Yaw RMSE [°]	15.12	14.23	14.88
Yaw error 95% [°]	29.62	28.38	28.11
Yaw error maximum [°]	37.09	34.39	39.41

It is clearly seen that the new weighting schemes offer a massive increase of accuracy both for horizontal error and yaw estimation. Yaw however can still not be fully trusted,

and it is by far the most inaccurate value estimated by the Kalman filter. The addition of GLONASS, it was hoped, would palliate this big error. As more satellites become available it should be easier to estimate the heading and the IMU bias affecting this measurement.

5.2.1. Addition Of GLONASS

The Novatel receiver data is then used in order to see the increase of accuracy obtained by the addition of GLONASS. As explained in Section 3.2. the Novatel receiver is higher end than the cheap U-Blox receiver. Table 5.3 presents the results of using only the GPS L1 data of the Novatel reference station. It also presents the accuracy results with and without the use of the filtering camera.

Table 5.3: Comparison between U-Blox data and Novatel (GPS L1 only)

	UBlox no camera	U-Blox camera	Novatel no camera	Novatel camera
Horizontal RMSE [m]	14.80	10.20	11.87	13.23
Horizontal error 95% [m]	27.79	25.67	22.15	23.09
Horizontal error maximum [m]	39.06	29.76	28.49	30.94
Yaw RMSE[°]	20.57	15.23	14.76	15.62
Yaw error 95% [°]	27.13	23.24	24.58	26.45
Yaw error maximum [°]	104.33	39.72	26.92	29.59
Mean number of satellites	6.54	4.61	5.00	4.40

The results from this table show us that the Novatel data has lower visibility of satellites than the U-Blox. The worst performance by the use of the camera and the fact that the mean number of satellites seen by the Novatel is also the same with and without the camera. This is attributed to the fact that the Novatel uses a high performance antenna, with high multipath resistance. The antenna filters the satellite before recording, and thus the available number of satellites is lower. Performance is reduced by the addition of the camera as it introduces some sources of error, as some times it detects clouds as buildings and blocks the satellites behind [6].

Once GLONASS satellites are added to the mixture, the increase in availability causes an increase in position and attitude accuracy. Table 5.4 shows the resulting accuracy caused by the use of the GLONASS constellation both in urban and suburban environment. Not only the horizontal accuracy is now up to a very accurate level, but also the yaw error. It was quite poor in the GPS only solution but now it is accurate and within reasonable limits. The error models respond well also to the GLONASS dataset (Table A.1 in the Appendix A).

5.2.1.1. Weighting of GLONASS measurements.

Section 4.1.1.4. introduced the lower accuracy of GLONASS satellites with respect to GPS. Small differences in the design of the system should make GLONASS satellites less precise. Different tests were done with different weighting factors, the most significant results are shown in Table 5.5. It can be seen that no weighting factor adds any advantage to

Table 5.4: Accuracy results for Novatel GPS/GLONASS (no camera) solution

	Urban	Suburban
Horizontal RMSE [m]	6.27	4.69
Horizontal error 95% [m]	11.40	7.73
Horizontal error maximum [m]	12.10	65.47
Yaw RMSE [°]	6.83	12.83
Yaw error 95% [°]	14.24	22.52
Yaw error maximum [°]	15.82	35.90
Mean number of satellites	8.66	11.78

the accuracy. The reason being that The weighting models applied already down weights GLONASS because of its lower C/N_0, making any additional weighting unnecessary.

Table 5.5: Novatel GLONASS weighting factors (no camera)

	no weighting	GPS only	GLONASS only	factor 1.3
Horizontal RMSE [m]	4.69	5.63	8.05	4.78
Horizontal error 95% [m]	7.73	9.20	38.73	7.83
Horizontal error maximum [m]	65.47	73.83	167.64	65.35
Yaw RMSE [°]	12.83	15.45	15.77	12.81
yaw error 95% [°]	22.52	26.80	30.44	22.88
yaw error maximum [°]	35.90	40.44	36.72	36.06

Different C/N_0 masks were applied, but they did not improve the results either. All tests where infructuous and no masking would increase the accuracy. This was also attributed to the fact that the Novatel data is already filtered. The mask is meant to offer additional blocking to NLOS satellites, yet the Novatel data set is already free of multipath influence.

5.3. Carrier-to-noise density masking

Once the satellite models have been presented, satellite masking is now applied. Satellite masking can work in conjunction with the presented models of previous sections. First, tests were done on a simple C/N_0 mask, in which a threshold is set and any satellite underneath it is discarded.

Several post processing runs were done to the algorithm with different C/N_0 mask thresholds in order to find the most optimal one. Figure 5.3. represents the histogram of C/N_0 values for all satellites. The camera is used to tell apart which satellites are LOS and which aren't. It was used as a visual guidance to where the most efficient threshold may lie. Thresholds around the $35dBHz$ were looked. The most optimal one being $34\ dbHz$. Table A.2 and Figure A.1 in the Appendix A shows all the values tested.

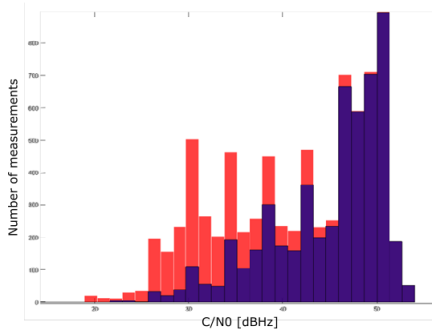

Figure 5.2: Histogram Carrier-to-Noise values. LOS satellites are in blue and NLOS in red

5.3.1. Correction Of The Camera

Figure 5.3. also revealed problems in the functioning of the camera. There are some low power satellites that are considered by the filter as LOS and also some high power satellites assigned as NLOS. This kind of errors degrade the solution like it was seen in Section 5.2.1.. In order to overcome this problems, an additional filter is added.This filter makes satellites above a certain threshold always be considered as LOS, while satellites below another threshold are considered as NLOS. The camera then only discriminates satellites with power levels between these two values. Several threshold were tested, the most effective ones being $37\ dBHz$ for the upper threshold and $33\ dBHz$ for the lower.

To check if it was working, the test of Section 5.2.1. was done again, applying this new filter. The results (Table 5.6) were that the U-Blox plus camera configuration became almost as precise as the Novatel single frequency solution.

Table 5.6: Comparison of Novatel GPS/GLONASS measurements without camera and camera plus carrier-to-noise filter

	No camera	Camera+ filter
Horizontal RMSE [m]	6.27	6.31
Horizontal error 95% [m]	11.40	11.45
Horizontal error maximum [m]	12.10	12.06
Yaw RMSE[°]	6.83	6.89
Yaw error 95% [°]	14.24	14.37
Yaw error maximum [°]	15.82	16.31

A clear conclusion can be extracted from this little test: A cheap U-Blox receiver plus the camera configuration can achieve the same performance as a Novatel receiver plus a high performance antenna. The Novatel is surely more accurate in duel configuration mode, yet it comes to show that the use of a camera to block NLOS signal has a lot of promise.

5.3.2. Different Doppler And Pseudorange Mask

Different masking threshold were set for both pseudorange and Doppler. A mask of 34 dBHz was set as the target reference. The Doppler mask was increased while the pseudorange was maintained.

Table 5.7: Different Doppler and pseudorange C/N0 masks for urban environment (U-Blox data)

Doppler mask/PR mask [dBHz]	34/34	36/33	39/31	32/36
Horizontal RMSE [m]	8.84	7.93	7.15	8.61
Horizontal error 95% [m]	17.46	14.84	13.83	15.28
Horizontal error maximum [m]	53.42	29.05	22.01	24.28
Yaw RMSE [°]	27.10	12.94	13.82	14.46
Yaw error 95% [°]	43.79	21.14	21.68	22.82
Yaw error maximum [°]	47.23	27.59	29.16	33.37

It can be seen that pseuodrange rate measurements are more affected than pseudorange measurement by multipath. However, although this concept did offer an improvement for the urban data set, it did not offer an increase in accuracy in the suburban (Table A.3 in the Appendix A).

This type of combination is also dependable on the models applied. Early test done with other models (Results seen in Table A.4 of the Appendix A) show that this concept does not always succeed. It is logic however, as the weighting factor might already act as mask in some situation. This concept should be further tested, as the data available is not enough.

5.4. Total Improvement

Once all these improvement are put together, the accuracy improves dramatically compared to the initial solution. Table 5.8 shows this progress for the Novatel GPS and GLONASS solution. The improvement for the suburban environments are in the Appendix A (Table A.5). The table show the increase caused by the use of different weighting models. A reduction of almost 50% in the position accuracy is achieved by the use of better weighting schemes, more suited for urban environments. The yaw error however, stays quite high. The addition of GLONASS in the final column of the table shows a reduction of yaw error to an acceptable level, and almost 50% from the original U-Blox measurements.

Table 5.8: Comparison of all the changes applied

	U-Blox (Old models)	U-Blox (new models + mask)	Novatel (GPS/GLONASS + models)
Horizontal RMSE [m]	14.80	7.15	6.27
Horizontal error 95% [m]	27.79	13.83	11.40
Horizontal error maximum [m]	39.06	22.01	12.10
Yaw RMSE [°]	20.57	13.82	6.83
Yaw error 95% [°]	27.13	21.68	14.24
Yaw error maximum [°]	104.33	29.16	15.82

Figure A.2 in the Appendix A shows the improvement for the U-Blox receiver accuracy.

CONCLUSIONS

This report set the objective to research and understand GNSS integration with INS. It also set to achieve palpable increases in the the positioning accuracy of a cheap INS/GNSS mix for positioning in urban areas.

The thesis started with the study of INS and GNSS positioning, first as a stand-alone and later as an integration. The Kalman filter has been studied as the integration technique. This integration allows for a much more accurate and continuous positioning, specially in urban environments, where a GNSS only solutions is prone to shortages.

The algorithm used by ENAC was studied, detecting those areas were imhprovement could be made. Position accuracy was good enough at the beginning, yet yaw estimation was unusable. In order to improve the estimation of the attitude it was thought that GLONASS should be added.

Also new weighting models were needed for the measurement covariance matrix. The current model was not strong enough and it was not doing a good job at blocking multipath signals.

The models, together with the implementation of GLONASS were tested using measurement taken in the city of Toulouse. The results evaluated showed that, indeed the weighting models were not adequate for urban environments. It could also be seen that GLONASS does make both the horizontal and yaw errors heavily reduced. The increased number of satellites does allow for a much better accuracy.

The addition of the weighting models and masks showed an improvement all combined showed an improvement of almost 50 % of the accuracy in the position for the U-Blox receiver. The yaw estimation, although heavily improved, was still not as good as it should. The addition of GLONASS did increase the accuracy of all parameters estimated. It must be taken into account however that the GLONASS measurement came from a Novatel receiver. Even though it was set in a single frequency configuration, it is still an expensive receiver capable of very accurate tracking.

The Novatel data can be used a reference of what could be achievable by a multi constellation, low cost receiver. It offers a target for performance in positioning and attitude estimation. The data offered by the Novatel also can be used as a target performance for the camera discrimination. The Novatel antenna definitively showed a high level of performance in blocking multipath. While examining the video taken by the camera it could be seen immediately that the antenna would work better than the camera. It makes sense to use the Novatel not only as a reference for positioning, speed and attitude, but also for satellite visibility.

Future work

In order to further increase the accuracy solution in urban environments using a cheap receiver more testing should be done with different weighting schemes. Although still useful, the performance of the used models change greatly between urban and suburban environments, and one can guess they would change even further if tested in open areas. The tests carried out in this thesis stayed in the urban environment of Toulouse and do not reflect a great variety. Toulouse has very low houses, four storey high. Cities with

urban canyons with higher building will experience even bigger errors, and so it even more powerful models would be needed.

Future work must be carried also to incorporate more constellation. At the end of this thesis it was not possible to incorporate neither Galileo nor Beidou. Although EGNOS pseudorange measurements were present, they could not be added either, as it is still not operational for positioning. It's ionospheric correction could still be applied though, which would definitely increase the accuracy of the solution heavily.

And effort should also be made into speeding up the algorithm. Although not mentioned in the thesis, the positioning algorithm was hardly faster than real time. After some improvement in the computations and cancelling almost all data recording, processing could be done faster than real time. Further improvement is possible and necessary for real-time use. Especially if both processing and recording is done at the same time by the same computer.

BIBLIOGRAPHY

[1] Groves, Paul D., *Principles of GNSS, inertial, and multisensor integrated navigation systems*, second edition, Artech House, London(2013). 3, 4, 16, 18, 21, 25, 27

[2] Navipedia *GNSS Market Report* [consulted: February 2015] Available: http://www.navipedia.net/index.php/GNSS_Market_Report. 4

[3] Inside GNSS *GNSS geodetic reference frames: consistency, stability and the related transformation parameters*[consulted: October 2014] Available: http://www.insight-gnss.org/workshop_presentations/220MZ20Reference.pdf. 4, 15

[4] Kaplan,Elliott D., Hegarty, Christopher J., *Understanding GPS: principles and applications*, Artech House, Noorwood, MA(2006). 4, 11, 25

[5] GPS.gov *GPS control segment*[consulted: March 2015] Available: http://www.gps.gov/systems/gps/control/. 6

[6] Gehrmann, Andreas, *Positioning in urban areas*, TU Berlin, Berlin(2014). 10, 26, 28, 37, 43

[7] Wikipedia *Orbital elements* [consulted: February 2015] Available: http://en.wikipedia.org/wiki/Orbital_elements. 12

[8] U.S government *GPS Interface Control Document*[consulted: October 2014] Available: http://www.gps.gov/technical/icwg/ ix, 12, 15

[9] UNSW Australia *Surveying and geospatial engineering* [consulted: February 2015] Available: http://www.sage.unsw.edu.au/snap/gps/gps_survey/chap6/642.htm 12

[10] UNAVCO *GLONASS Interface Control Document*[consulted: October 2014] Available: https://www.unavco.org/help/glossary/docs/ICD_GLONASS_5.1_28200829_en.pdf ix, 13, 14, 15, 30

[11] Carcanague, Sebastien *Low-cost GPS/GLONASS Precise Positioning Algorithm in Constrained Environment*, Universite de Toulouse, Toulouse(2013). 14, 31, 37, 38

[12] Wikipedia *BeiDou Navigation Satellite System* [consulted: October 2014] Available: http://en.wikipedia.org/wiki/BeiDou_Navigation_Satellite_System 15

[13] Navipedia *BeiDou B1 Band* [consulted: February 2014] Available: http://www.navipedia.net/index.php/BeiDou_Signal_Plan ix, 16

[14] European Comision *Galileo Interface Control Document*[consulted: October 2014] Available: http://ec.europa.eu/enterprise/policies/satnav/galileo/open-service/index_en.htm 16

[15] EGNOS Open Service Document *EGNOS open service: Performance requirements* [consulted: February 2015] Available: http://www.navipedia.net/index.php/EGNOS_Open_Service

[16] Changdon, Kee, Parkinson, Bradford W. "Wide Area Differential GPS (WADGPS): Future Navigation System" *IEEE TRANSACTIONS ON AEROSPACE AND ELECTRONIC SYSTEMS* VOL. 32, NO. 2 APRIL 1996.

[17] Beidou *Beidou Interface Control Document*[consulted: October 2014] Available: http://www.beidou.gov.cn/attach/2013/12/26/20131226b8a6182fa73a4ab3a5f107f762283712.pdf 16

[18] UBlox *EVK-6T specifications*[consulted: October 2014] Available: http://www.u-blox.com/en/evaluation-tools-a-software/gps-evaluation-kits/evk-6-evaluation-kits.html 27

[19] xSens *xSense MTi specifications*[consulted: October 2014] Available: https://www.xsens.com/products/mti/ 27

[20] Novatel *Novatel SPAN specifications*[consulted: October 2014] Available: http://www.novatel.com/products/span-gnss-inertial-systems/ 28

[21] Wikipedia *Clock Synchronization*[consulted: October 2014] Available: http://en.wikipedia.org/wiki/Clock_synchronization 28

[22] IDS *uEye camera specifications*[consulted: October 2014] Available: https://en.ids-imaging.com/video_ueye.html 28

[23] Furuno *Furuno VN-870 specifications*[consulted: January 2015] Available: http://www.furuno.com/en/products/gnss-chip/ePV7010B 28

[24] Liang Heng, Grace Xingxin Gao, Todd Walter, and Per Enge, "Statistical Characterization of GLONASS Broadcast Ephemeris Errors", *Proceedings of the 24th International Technical Meeting of The Satellite Division of the Institute of Navigation*, 3109 - 3117, 2011. 30, 39

[25] gAGE UPC *GLONASS Navigation RINEX 2.10 Format* [consulted: December 2014] Available: http://gage14.upc.es/gLAB/HTML/GLONASS_Navigation_Rinex_v2.11.html 31

[26] Navipedia *Ionospheric models for single frequency receivers* [consulted: February 2015] Available: http://www.navipedia.net/index.php/Ionospheric_Models_for_Single_Frequency_Receivers 31

[27] gAGE UPC *Observation RINEX 2.11 Format* [consulted: December 2014] Available: http://gage14.upc.es/gLAB/HTML/Observation_Rinex_v2.11.html 32

[28] gAGE UPC *SBAS Navigation RINEX 3.01 Format* [consulted: February 2015] Available: http://gage14.upc.es/gLAB/HTML/SBAS_Navigation_Rinex_v3.01.html

[29] Petovello, Mark "Carrier-to-noise density and AI for INS/GPS integration" *Inside GNSS*, 20-29, September 2009 33

[30] Navipedia *Correlators* [consulted: February 2015] Available: http://www.navipedia.net/index.php/Correlators 34

[31] Kuusniemi, Heidi, *User level reliability and quality monitoring in satellite based personal navigation*, Tampere University of Technology, Tampere (2005). 37, 38

APPENDIX A. RESULT TABLES AND FIGURES

Table A.1: Weighting models Applied to Novatel's GPS/GLONASS solution (no camera)

Models applied to GLONASS	old models	PR model	PR + Doppler model
Horizontal RMSE [m]	7.57	7.23	6.27
Horizontal error 95% [m]	15.40	14.82	11.40
Horizontal error maximum [m]	19.80	19.45	12.10
Yaw RMSE [°]	10.86	10.50	6.83
Yaw error 95% [°]	23.61	22.97	14.24
Yaw error maximum [°]	25.85	25.30	15.82

Table A.2: Different masking values for U-Blox receiver (no camera)

Mask value [dBHz]	none	30	33	35	37	40
Horizontal RMSE [m]	11.09	9.98	9.14	9.42	10.49	53.84
Horizontal error 95% [m]	22.72	20.20	18.34	19.04	22.12	101.94
Horizontal error maximum [m]	34.25	46.45	25.64	26.05	43.87	695.64
Yaw RMSE [°]	16.82	15.54	16.22	16.09	17.85	174.28
Yaw error 95% [°]	34.89	30.49	32.65	32.62	36.51	-
Yaw error maximum [°]	43.14	41.39	42.43	43.04	46.22	-

Table A.3: Different Doppler and pseudorange C/N_0 masks for suburban environment with the U-Blox receiver and the new models applied (no camera)

Doppler mask/PR mask	34/34	31/37	39/31
Horizontal RMSE [m]	6.22	6.23	6.14
Horizontal error 95% [m]	11.25	12.13	10.48
Horizontal error maximum [m]	35.90	34.81	36.66
Yaw RMSE [°]	6.86	7.49	6.79
Yaw error 95% [°]	17.52	19.50	17.67
Yaw error maximum [°]	56.13	51.95	41.17

Table A.4: Different pseudrange and Doppler masking using the old weighting model in the U-Blox receiver (no camera)

Doppler mask /PR mask	35/35	35/33	35/34	34/34	34/35	33/35	33/33
Horizontal RMSE [m]	9.33	9.15	9.14	9.07	9.28	9.34	9.19
Horizontal error 95% [m]	17.57	16.62	16.80	16.63	17.36	17.53	16.93
Horizontal error maximum [m]	25.15	25.43	25.23	25.09	24.85	24.79	25.12
Yaw RMSE [°]	16.12	16.29	16.49	16.61	16.27	16.28	16.14
Yaw error 95% [°]	28.05	28.07	28.45	27.31	27.51	27.85	27.31
Yaw error maximum [°]	33.13	33.15	33.47	32.54	32.77	32.48	32.04

Table A.5: Total improvement for the suburban environment

	U-Blox (Old models)	U-Blox (new models + mask)	Novatel (GPS/GLONASS + models)
Horizontal RMSE [m]	6.84	6.09	4.69
Horizontal error 95% [m]	16.57	11.66	7.73
Horizontal error maximum [m]	29.68	22.35	65.47
Yaw RMSE [°]	15.12	14.88	12.83
Yaw error 95% [°]	29.62	28.11	22.52
Yaw error maximum [°]	37.09	39.41	35.90

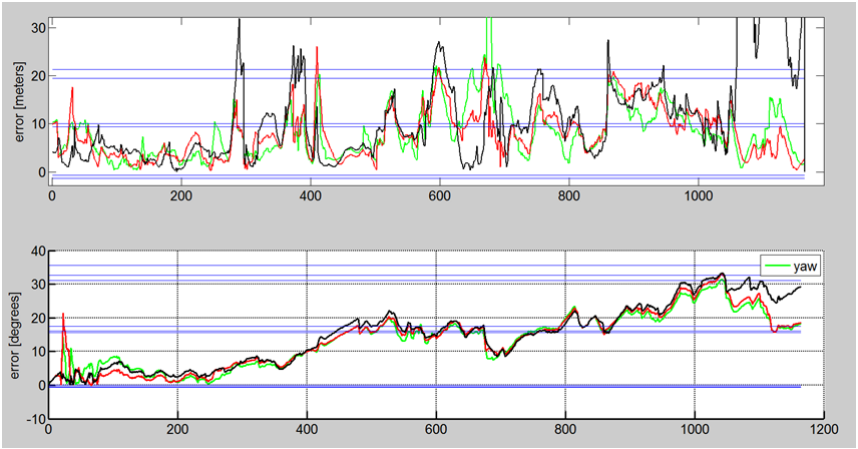

Figure A.1: Comaprison of C/N_0 masks. 30 dBHz (green),35 dBHz (red),40 dBHz (black)

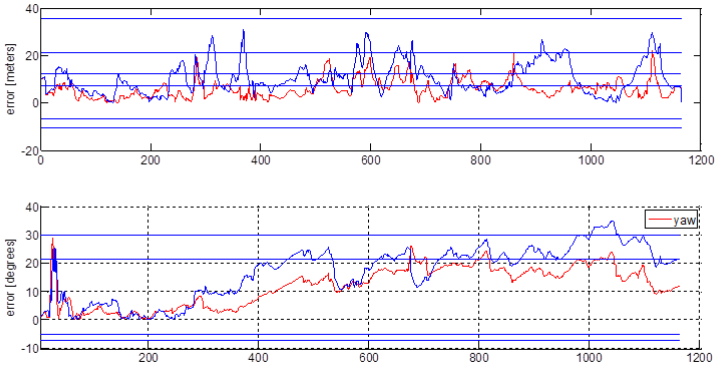

Figure A.2: Total improvement: Old system (blue),New system (red)

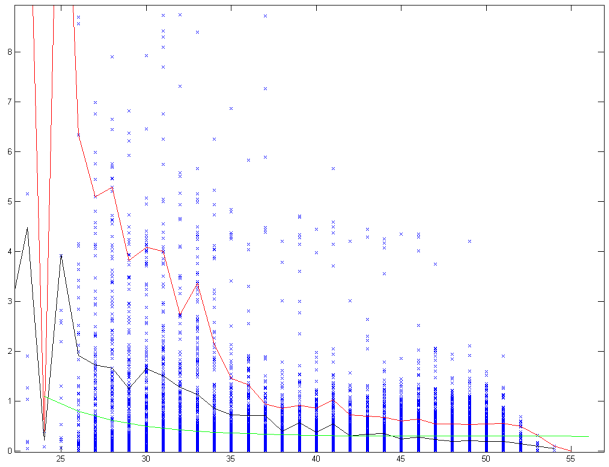

Figure A.3: Distribution of pseudorange rate error

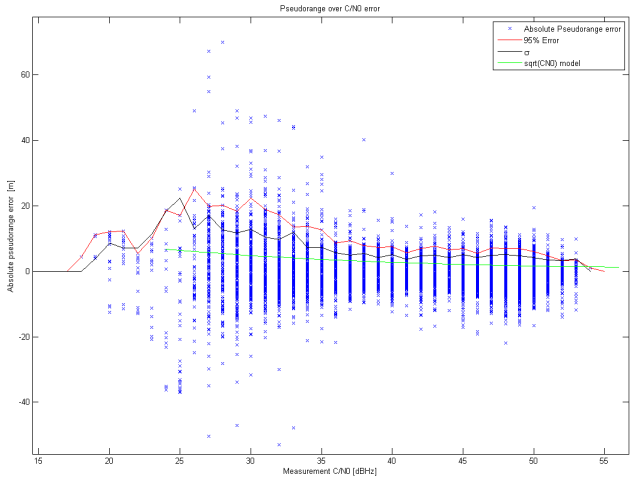

Figure A.4: Distribution of pseudorange error